Research Square

Preprints are preliminary reports that have not undergone peer review.
They should not be considered conclusive, used to inform clinical practice,
or referenced by the media as validated information.

# Engineering Kluyveromyces marxianus for high-titer succinic acid production at elevated temperature and low pH from sugarcane bagasse hemicellulose hydrolysate and crude biodiesel glycerol

**Ashokkumar Kumaravel**

bioashok00793@gmail.com

SR University

**Likha Chandran**

VNR Vignana Jyothi Institute of Engineering and Technology, Nizampet (S.O)

**Prasad shanmughan**

SRM Institute of Science and Technology

**Research Article**

**Keywords:** Kluyveromyces marxianus, succinic acid, crude biodiesel glycerol, reductive TCA pathway, NADH cofactor engineering, lignocellulosic hydrolysate

**Posted Date:** November 23rd, 2026

**DOI:** https://doi.org/10.21203/rs.3.rs-11716461/v1

**License:** This work is licensed under a Creative Commons Attribution 4.0 International License.
Read Full License

**Additional Declarations:** No competing interests reported.

**Engineering *Kluyveromyces marxianus* for high-titer succinic acid production at elevated temperature and low pH from sugarcane bagasse hemicellulose hydrolysate and crude biodiesel glycerol**

Ashokkumar Kumaravel[1,2]*, Likha Chandran[3], Prasad shanmughan[4].

[1]School of Science and Humanities, Department of Biotechnology, SR University, Warangal, India.

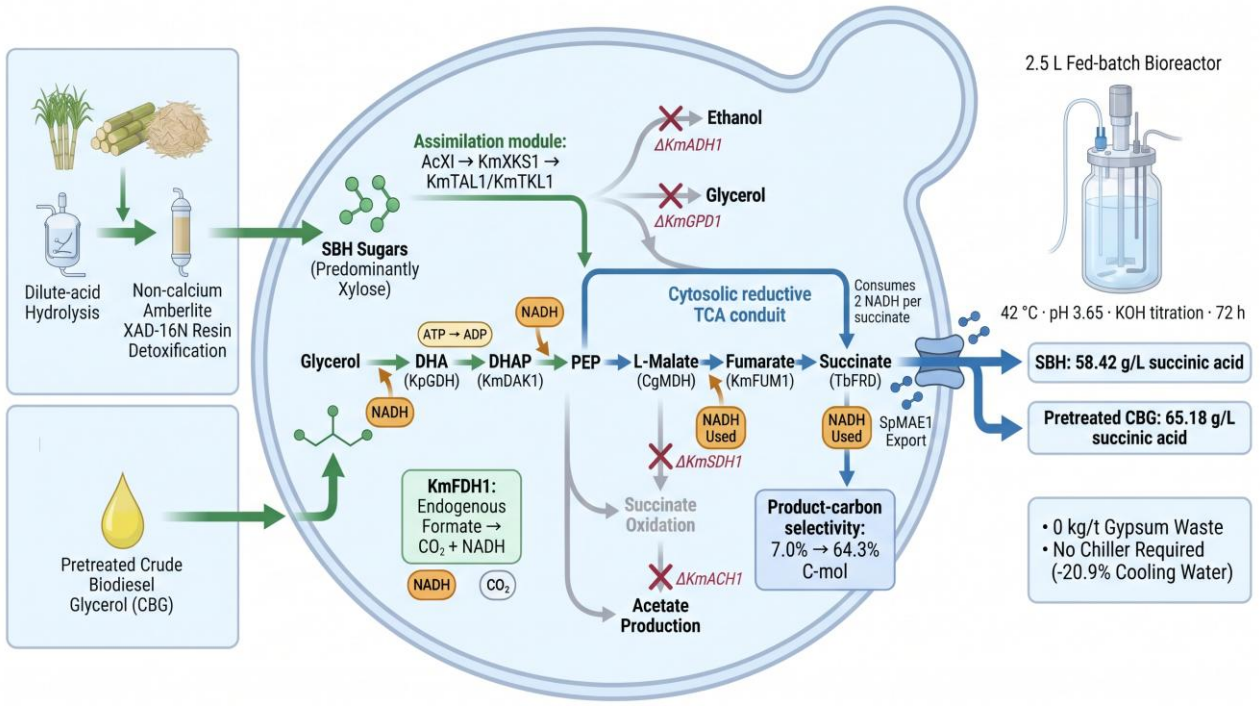
[2]Centre for Research and Innovation, Academy of Maritime Education and Training (AMET) Deemed to Be University, Kanathur, Chennai 603112, Tamil Nadu, India.

[3]Department of Chemistry, VNR Vignana Jyothi Institute of Engineering and Technology, Vignana Jyothi Nagar, Pragathi Nagar, Nizampet (S.O), Hyderabad, Telangana, India.

[4]IISM, SRM institute of Science and Technology. Tamilnadu, India.

Corresponding author: Ashokkumar Kumaravel (bioashok00793@gmail.com)

## Graphical Abstract



## Highlights

- Thermotolerant, acidotolerant *Kluyveromyces marxianus* engineered for low-pH succinate production at 42 °C and pH 3.65
- 58.42 g/L succinic acid from bagasse hemicellulose hydrolysate and 65.18 g/L from pretreated crude biodiesel glycerol
- KOH titration at pH 3.65 eliminates solid gypsum sludge (0 vs 1,458 kg/t) and reduces base/acid demand by 78.0 %
- Fermentation at 42 °C removes mechanical refrigeration (113.7 $kWh_e$/t broth) and lowers cooling-water demand by 20.9 %
- Product-carbon selectivity raised from 7.0 to 64.3 % C-mol by sequential deletion of KmADH1, KmGPD1, KmSDH1 and KmACH1

**Abstract**

Succinic acid is a high-priority platform chemical, yet industrial biomanufacturing is constrained by fermentation cooling duty, stoichiometric base neutralisers, and downstream calcium sulfate (gypsum) sludge. Here, thermotolerant, acidotolerant yeast *Kluyveromyces marxianus* was engineered for reductive tricarboxylic acid (rTCA) succinic acid production from non-food residues at 42 °C and pH 3.65. Integrating *Actinobacillus succinogenes* PEP carboxykinase (AsPCK), *Corynebacterium glutamicum* malate dehydrogenase (CgMDH), native fumarase (KmFUM1), *Trypanosoma brucei* NADH-dependent fumarate reductase (TbFRD), and *Schizosaccharomyces pombe* dicarboxylate exporter (SpMAE1) established the synthetic conduit. Sequential CRISPR/Cas9 disruption of *KmADH1*, *KmGPD1*, *KmSDH1*, and *KmACH1* suppressed ethanol and glycerol overflow and converted acetate excretion into net uptake, raising succinic acid titre by 97.6% (2.51 to 4.96 g/L) and product-carbon selectivity from 7.0% to 64.3% C-mol on hydrolysate. Non-calcium Amberlite XAD-16N detoxification of sugarcane bagasse hemicellulose hydrolysate (SBH) avoided upstream gypsum, while *Acidothermus cellulolyticus* xylose isomerase (AcXI) with *KmXKS1*, *KmTAL1*, and *KmTKL1* enabled pentose assimilation. In 2.5 L bioreactors (42 °C, pH 3.65, KOH titration), the strain produced 23.50 g/L in batch (18 h) and 58.42 g/L in fed-batch (72 h; 0.379 g/g yield; 0.811 g/L/h). Glycerol-fed cultures combining *Klebsiella pneumoniae* glycerol dehydrogenase (KpGDH) and *KmDAK1* with rTCA amplification expanded whole-cell NADH by 145.2% (1.15 to 2.82 μmol/g DCW), reaching 71.20 g/L on pure glycerol (0.486 g/g) and 65.18 g/L on crude biodiesel glycerol (0.463 g/g). KOH titration at pH 3.65 eliminates gypsum (0 vs 1,458 kg/t) and cuts base/acid demand by 78.0%, while 42 °C operation removes mechanical chilling (113.7 $kWh_e$/t) and saves 20.9% cooling water.

**Keywords:** *Kluyveromyces marxianus*; succinic acid; crude biodiesel glycerol; reductive TCA pathway; NADH cofactor engineering; lignocellulosic hydrolysate

## 1. Introduction

The environmental pressures created by fossil fuel depletion, petrochemical manufacturing and persistent plastic pollution have driven efforts to build carbon-neutral biorefineries that produce platform chemicals and bio-based polymers from renewable biomass (Beauprez et al. 2010; Nielsen and Keasling 2016). Succinic acid (butanedioic acid, $C_4H_6O_4$) carries two terminal carboxyl groups and is therefore a versatile $C_4$ building block (Beauprez et al. 2010; Choi et al.

2016). Catalytic conversion gives 1,4-butanediol, tetrahydrofuran, γ-butyrolactone, adipic acid, 2-pyrrolidone and biodegradable poly(butylene succinate) (Bozell and Petersen 2010; Li et al. 2010), and succinic acid has been consistently ranked among the top value-added bio-based chemicals in US Department of Energy assessments (Bozell and Petersen 2010; Straathof 2014). Its biotechnological production has been reviewed extensively (Cheng et al. 2012). Microbial succinate production follows three primary architectures: the oxidative tricarboxylic acid (TCA) cycle, the glyoxylate shunt, and the reductive TCA (rTCA) branch (Beauprez et al. 2010; López-Garzón and Straathof 2014). Under fully aerobic conditions the oxidative route converts acetyl-CoA to succinate through citrate, isocitrate and α-ketoglutarate, releasing two moles of $CO_2$ per turn and capping the molar yield at 1.0 mol succinate per mol hexose (0.656 g/g) (Beauprez et al. 2010; López-Garzón and Straathof 2014). The glyoxylate shunt bypasses both oxidative decarboxylations via isocitrate lyase but still loses carbon at pyruvate dehydrogenase and is subject to glucose repression (Beauprez et al. 2010; Gao et al. 2016). The rTCA branch is carbon-conserving: phosphoenolpyruvate (PEP) or pyruvate is carboxylated to oxaloacetate (OAA) with fixation of $CO_2$, then reduced to L-malate, dehydrated to fumarate and reduced to succinate (Beauprez et al. 2010; Borges and Pereira 2011). On a carbon-stoichiometric basis (when external reducing power such as $H_2$ is supplied), the pathway allows 2.0 mol succinate per mol hexose (1.67 mol per mol pentose, 1.311 g/g); on carbohydrates alone without an external electron donor, electron conservation between hexose or pentose (degree of reduction $\gamma = 4.0$ per carbon, 24 $e^-$ per hexose) and succinic acid ($\gamma = 3.5$ per carbon, 14 $e^-$ per mol) sets the maximum redox-balanced stoichiometric yield at 1.714 mol/mol hexose (1.429 mol/mol pentose), corresponding to 1.124 g/g from either glucose or xylose (Beauprez et al. 2010; Yuzbashev et al. 2010). Because the rTCA branch consumes two moles of NADH per mole of succinate formed from OAA (OAA + 2 NADH + 2 $H^+$ → succinate + 2 $NAD^+$ + $H_2O$), whereas glycolysis to two moles of PEP generates only two moles of NADH per hexose, rTCA flux on sugars is strictly constrained by cytosolic NADH availability (Borges and Pereira 2011; Cui et al. 2017). Despite progress in *Escherichia coli*, *Actinobacillus succinogenes* and *Mannheimia succiniciproducens*, two technoeconomic bottlenecks persist: fermentation cooling and organic-acid neutralisation with its downstream salt burden (López-Garzón and Straathof 2014; Straathof 2014). Aerobic metabolism and mechanical agitation are strongly exothermic, and mesophilic hosts operated at 28-30 °C require chilled-water refrigeration, which can account for 15-30 % of utility operating expenditure in warm climates (Abdel-Banat et al. 2010; Baptista and Domingues 2022). Operating at 37-42 °C widens the

temperature approach between broth and ambient cooling-tower water and allows direct heat rejection without mechanical chillers (Abdel-Banat et al. 2010; Baptista and Domingues 2022). In parallel, succinate-producing bacteria are constrained to pH 6.5-7.0 by acid sensitivity (Beauprez et al. 2010; Yuzbashev et al. 2010) and are commonly neutralised with $Ca(OH)_2$ or $CaCO_3$. Acidifying divalent calcium succinate with $H_2SO_4$ precipitates 1.46 kg of calcium sulfate dihydrate (gypsum) per kg of free acid recovered (López-Garzón and Straathof 2014; Yuzbashev et al. 2010); a 50,000 t/year plant therefore generates roughly 73,000 t of gypsum sludge annually (López-Garzón and Straathof 2014; Yuzbashev et al. 2010). The thermotolerant, acidotolerant non-conventional yeast *Kluyveromyces marxianus* is an attractive alternative platform: it is among the fastest-growing eukaryotes ($\mu > 0.6\ h^{-1}$), grows vigorously at 40-45 °C, tolerates pH 3.0-4.5, and resists furfural, 5-hydroxymethylfurfural (5-HMF) and aliphatic weak acids (Lane and Morrissey 2010; Nonklang et al. 2008). Commercial viability also requires low-cost, non-food feedstocks rather than refined sugars (Jönsson and Martín 2016; Nielsen and Keasling 2016).

Two abundant and complementary agro-industrial residues were examined here: sugarcane bagasse hemicellulose hydrolysate (SBH) and crude biodiesel glycerol (CBG). Bagasse is the fibrous residue of sugarcane crushing, with global annual production above 540 million tonnes (Borges and Pereira 2011; Jönsson and Martín 2016); its dilute-acid hemicellulose hydrolysate is rich in pentoses, mainly D-xylose with minor D-glucose and L-arabinose (Borges and Pereira 2011; Jönsson and Martín 2016). To avoid the upstream gypsum generated by calcium hydroxide overliming, a non-calcium polymeric resin adsorption process (Amberlite XAD-16N) was implemented. For pentose assimilation, a thermotolerant xylose isomerase from *Acidothermus cellulolyticus* (AcXI) was integrated with native xylulokinase (KmXKS1) and overexpression of the non-oxidative pentose phosphate pathway (KmTAL1, KmTKL1) (Ledesma-Amaro et al. 2016; Wang et al. 2013). Crude glycerol is the principal liquid co-product of fatty acid methyl ester (biodiesel) transesterification, generated at roughly 100 kg per tonne of biodiesel, and contains residual methanol, ash and free fatty acids (Gao et al. 2016; Zhu et al. 2014). Glycerol is a more reduced carbon source (degree of reduction $\gamma = 4.67$ per carbon, 14 $e^-$ per mol) than hexoses or pentoses ($\gamma = 4.0$). Oxidising one mole of glycerol to dihydroxyacetone (DHA) via $NAD^+$-dependent glycerol dehydrogenase generates one mole of cytosolic NADH; subsequent ATP-dependent phosphorylation of DHA to dihydroxyacetone phosphate (DHAP) by dihydroxyacetone kinase followed by lower glycolytic oxidation of triose phosphate to PEP via glyceraldehyde-3-phosphate dehydrogenase generates a second mole of cytosolic NADH.

Converting one mole of glycerol to PEP therefore supplies exactly two moles of cytosolic NADH, matching the two moles consumed per mole of succinate in the rTCA branch and making glycerol + $CO_2$ → succinic acid a stoichiometrically redox-neutral conversion with a theoretical mass yield of 1.282 g/g (1.0 mol/mol) (Cui et al. 2017; Yuzbashev et al. 2010). Here *K. marxianus* was engineered for succinic acid production at 42 °C and pH 3.65 from SBH and CBG (Fig. 1A). First, the cytosolic rTCA conduit was assembled from AsPCK, CgMDH, native KmFUM1, TbFRD and SpMAE1. Second, sequential CRISPR/Cas9 editing disrupted four competing carbon and redox sinks: alcohol dehydrogenase 1 (KmADH1), glycerol-3-phosphate dehydrogenase 1 (KmGPD1), succinate dehydrogenase flavoprotein subunit 1 (KmSDH1) and acetyl-CoA hydrolase 1 (KmACH1). Third, pentose catabolism was installed via AcXI, KmXKS1, KmTAL1 and KmTKL1. Fourth, an oxidoreductive glycerol-assimilation module (KpGDH, KmDAK1) and endogenous formate dehydrogenase (KmFDH1) were combined with copy-number amplification of the rTCA sink. Fed-batch fermentation in 2.5 L bioreactors at pH 3.65 with KOH titration reached 58.42 g/L on SBH and 65.18 g/L on CBG at 42 °C. The complete process train, reconciled mass and carbon balances, and cooling and neutralisation energetics are reported.

## 2. Materials and methods

### 2.1. Microorganisms, media and culture conditions

Strains and plasmids are listed in Table 1. *Escherichia coli* DH5α was used for plasmid propagation and recombinant DNA work, cultured at 37 °C in Lysogeny Broth (10 g/L tryptone, 5 g/L yeast extract, 10 g/L NaCl) supplemented with 100 µg/mL ampicillin. The parental chassis was the thermotolerant industrial strain *K. marxianus* KM-WT (derived from the *K. marxianus* NBRC 1777 / DMKU3-1042 industrial lineage (Baptista and Domingues 2022; Nonklang et al. 2008)). A uracil-auxotrophic derivative, KM-01U, carrying a complete coding-sequence deletion of orotidine-5'-phosphate decarboxylase (Δura3), was constructed by homologous recombination with 400 bp direct-repeat flanks and counter-selected on synthetic complete agar containing 1.0 g/L 5-fluoroorotic acid (Baptista and Domingues 2022; Nonklang et al. 2008). Yeast strains were maintained on YPD (10 g/L yeast extract, 20 g/L peptone, 20 g/L D-glucose) at 30, 37 or 42 °C with orbital agitation at 220 rpm. Synthetic complete drop-out medium (SC-Ura) contained 6.7 g/L yeast nitrogen base without amino acids, 1.92 g/L uracil-free drop-out supplement and 20 g/L D-glucose, D-xylose or glycerol. Solid media contained 20 g/L agar. Pentose and glycerol seed

and flask fermentations used YPX (10 g/L yeast extract, 20 g/L peptone, 20–50 g/L D-xylose) and YPG (10 g/L yeast extract, 20 g/L peptone, 20–50 g/L pure or pretreated crude glycerol).

### 2.2. Feedstock preparation and non-calcium detoxification

#### 2.2.1. Sugarcane bagasse hemicellulose hydrolysate

Sugarcane bagasse was collected from an industrial sugar refinery, knife-milled to pass a 20-40 mesh screen, washed with deionised water and oven-dried at 65 °C to constant weight. Dilute-acid hydrolysis was carried out in a 5 L Hastelloy C-276 reactor at a solid-to-liquid ratio of 1:8 (w/v) with 1.2 % (w/v) $H_2SO_4$ at 135 °C for 45 min under mechanical agitation at 150 rpm (Borges and Pereira 2011; Jönsson and Martín 2016). After rapid cooling, the insoluble cellolignin pulp was removed by vacuum filtration. Calcium hydroxide overliming was deliberately avoided. Instead, the acidic filtrate was adjusted to pH 5.5 with 5 M KOH and passed through a jacketed glass column packed with macroporous non-ionic polymeric adsorbent resin at 1.5 bed volumes per hour, followed by polishing with 1.0 % (w/v) activated charcoal at 50 °C for 45 min to remove furan aldehydes and phenolic aromatics without calcium sulfate precipitation. The clarified SBH contained 74.2 ± 2.0 g/L D-xylose, 12.8 ± 0.4 g/L D-glucose, 7.1 ± 0.3 g/L L-arabinose (94.1 ± 2.1 g/L total reducing sugars), 4.4 ± 0.2 g/L acetic acid, 0.38 ± 0.03 g/L furfural and 0.14 ± 0.02 g/L 5-HMF. For fed-batch feeding, clarified SBH was concentrated under reduced pressure (55 °C, 90 mbar) and supplemented with corn steep liquor (CSL) to yield a concentrated feed containing 340.0 g/L total sugars (265.0 g/L D-xylose, 45.0 g/L D-glucose, 25.0 g/L L-arabinose, 5.0 g/L minor oligomers), 14.2 g/L acetic acid and 60.0 g/L CSL.

#### 2.2.2. Crude biodiesel glycerol

Crude biodiesel glycerol (CBG) was obtained from a commercial fatty acid methyl ester plant operating on used cooking oil. The raw material contained 81.5 ± 1.8 % (w/w) glycerol, 4.5 ± 0.3 % (w/w) methanol, 5.4 ± 0.3 % (w/w) inorganic ash, 2.4 ± 0.2 % (w/w) matter organic non-glycerol (MONG) and 6.2 ± 0.4 % (w/w) moisture at pH 10.2 ± 0.3 (Gao et al. 2016; Zhu et al. 2014). Undiluted raw CBG was acidified to pH 2.0 with concentrated $H_2SO_4$ (6 M) to protonate soaps and separate free fatty acids and MONG, which were decanted as the upper organic phase. Residual methanol and volatiles were stripped by rotary vacuum evaporation at 60 °C and 80 mbar to below 0.01 g/L. The dense glycerol-rich phase was neutralised to pH 6.0 with 5 M KOH, adjusted to a standardised working stock density with deionised water, and clarified by

centrifugation at 10,000 × g for 20 min. The resulting clarified CBG feed stock contained 785.0 ± 19.0 g/L (78.5 ± 1.9 % w/v) glycerol, 18.0 ± 1.0 g/L residual organic acids/salts and 32.0 ± 2.0 g/L ash at pH 6.0 ± 0.1. For shake-flask and batch media, this clarified 785.0 g/L CBG stock was diluted directly into medium to provide the specified initial glycerol concentration (20.0 or 50.0 g/L in shake flasks; 55.0 g/L in initial bioreactor batches).

### 2.3. Plasmid construction and genetic engineering

All oligonucleotide primers, CRISPR protospacers and overlap-extension knockout donor primers are listed in Table S1. Heterologous and synthetic coding sequences were codon-optimised for *K. marxianus* and chemically synthesised (Table S3): *A. succinogenes* PEP carboxykinase (AsPCK, 538 aa, 1,617 bp, modelled on UniProt A6VKV4), *C. glutamicum* malate dehydrogenase (CgMDH, 328 aa, 987 bp, modelled on UniProt Q8NN33), *T. brucei* glycosomal NADH-dependent fumarate reductase (TbFRD, 1,142 aa, 3,429 bp, modelled on UniProt Q57W38 / locus Tb927.5.930), *A. cellulolyticus* thermostable xylose isomerase (AcXI, 407 aa, 1,224 bp, modelled on UniProt A0LWM6), *S. pombe* $C_4$-dicarboxylate transporter (SpMAE1, 438 aa, 1,317 bp, modelled on UniProt P50537), *K. pneumoniae* $NAD^+$-dependent glycerol dehydrogenase, *K. marxianus* dihydroxyacetone kinase (KmDAK1, 588 aa, 1,767 bp, locus KLMA_30184) and *K. marxianus* $NAD^+$-dependent formate dehydrogenase. Complete nucleotide sequences are provided in Table S3, and all gene-specific amplification primers in Table S1 match the 5’ and 3’ termini of the Table S3 coding sequences identically.

CRISPR/Cas9 genome editing used a *Streptococcus pyogenes* Cas9 (Hsu et al. 2013) driven by the constitutive PKmTEF1 promoter and terminated by TScCYC1, integrated at the fcy1 locus of KM-01U to yield the editing chassis KM-Cas9. Guide RNAs (20-nt protospacers) targeting KmADH1, KmGPD1, KmSDH1 and KmACH1 were designed using CRISPOR (Haeussler et al. 2016) against NGG protospacer-adjacent motifs with zero predicted off-target sites in the *K. marxianus* genome (Table S1). Each sgRNA cassette was expressed from the RNA polymerase III promoter PKmSNR52 and fused at its 3’ end to a self-cleaving hepatitis delta virus (HDV) ribozyme (Haeussler et al. 2016; Hsu et al. 2013). Markerless homology-directed repair (HDR) donor cassettes were generated by overlap-extension PCR uniting 500 bp upstream (5’-UTR) and 500 bp downstream (3’-UTR) flanking arms via a 30 bp complementary fusion junction (primers -del-UP-F/FUS-R and -del-FUS-F/DN-R, Table S1). Multi-gene integration cassettes were assembled using strong endogenous promoters (PKmTDH3, PKmPGK1, PKmGAP,

PKmENO1 and PKmTEF1) with NEBuilder HiFi DNA Assembly Master Mix. Competent yeast cells were transformed by electroporation (1.5 kV, 25 μF, 200 Ω, 0.2 cm cuvette; Bio-Rad Gene Pulser Xcell). Transformants were selected on SC-Ura plates, verified by diagnostic colony PCR and Sanger sequencing, and subjected to 5-FOA counterselection (1.0 g/L) after each integration step to excise the direct-repeat-flanked KmURA3 marker prior to subsequent transformations (Table 1).

**Table 1. Strains and plasmids used in this study.**

| Strain / plasmid | Genotype / key characteristics | Source |
|---|---|---|
| **pKM-Cas9-Ura** | AmpR, PKmTEF1-SpCas9-TScCYC1 integrative vector, recyclable KmURA3 marker | This study |
| **pCR-KmADH1** | PKmSNR52-sgRNA(KmADH1)-HDV ribozyme in pKM-Cas9-Ura | This study |
| **pCR-KmGPD1** | PKmSNR52-sgRNA(KmGPD1)-HDV ribozyme in pKM-Cas9-Ura | This study |
| **pCR-KmSDH1** | PKmSNR52-sgRNA(KmSDH1)-HDV ribozyme in pKM-Cas9-Ura | This study |
| **pCR-KmACH1** | PKmSNR52-sgRNA(KmACH1)-HDV ribozyme in pKM-Cas9-Ura | This study |
| **pXI-XKS** | PKmGAP-AcXI-TKmCYC1, PKmENO1-KmXKS1-TKmADH1, recyclable KmURA3 | This study |
| **pPPP-Up** | PKmTEF1-KmTAL1-TKmTEF1, PKmPGK1-KmTKL1-TKmPGK1, recyclable KmURA3 | This study |
| **pSA-rTCA** | PKmTDH3-AsPCK-TKmCYC1, PKmPGK1-CgMDH-TKmADH1, recyclable KmURA3 | This study |
| **pSA-FRD-MAE** | PKmGAP-TbFRD-TKmTEF1, PKmENO1-SpMAE1-TKmPGK1, recyclable KmURA3 | This study |
| **pGLY-GDH** | PKmTDH3-KpGDH-TKmCYC1, recyclable KmURA3 | This study |
| **pGLY-DAK-MAE** | PKmPGK1-KmDAK1-TKmADH1, PKmENO1-SpMAE1-TKmPGK1, recyclable KmURA3 | This study |
| **pGLY-FDH** | PKmTEF1-KmFDH1-TKmTEF1, recyclable KmURA3 | This study |
| **E. coli DH5α** | $F^-$ endA1 glnV44 thi-1 recA1 gyrA96 relA1 deoR nupG Φ80dlacZΔM15 | Lab stock |
| **KM-WT** | Wild-type thermotolerant, acidotolerant *K. marxianus* (NBRC 1777 / DMKU3-1042 lineage) | Lab stock (Nonklang et al. 2008) |
| **KM-01U** | KM-WT Δura3 (homologous recombination, 5-FOA counter-selected) | This study |
| **KM-Cas9** | KM-01U fcy1::(PKmTEF1-SpCas9-TScCYC1), URA3 recycled (5-FOA) | This study |
| **KM-X01** | KM-Cas9 integrated with pXI-XKS (AcXI, KmXKS1), | This study |

| | | |
|---|---|---|
| | URA3 recycled (5-FOA) | |
| **KM-X02** | KM-X01 integrated with pPPP-Up (KmTAL1, KmTKL1), URA3 recycled (5-FOA) | This study |
| **KM-SA01** | KM-X02 sequentially integrated with pSA-rTCA (URA3 recycled) and pSA-FRD-MAE | This study |
| **KM-SA02** | KM-SA01 with URA3 recycled on 1.0 g/L 5-FOA | This study |
| **KM-SA03** | KM-SA02 ΔKmadh1 (markerless HDR, URA3 cured) | This study |
| **KM-SA04** | KM-SA03 ΔKmgpd1 (markerless HDR, URA3 cured) | This study |
| **KM-SA05** | KM-SA04 ΔKmsdh1 (markerless HDR, URA3 cured) | This study |
| **KM-SA06** | KM-SA05 ΔKmach1 (quadruple knockout, SBH production chassis, URA3 cured) | This study |
| **KM-G01** | KM-SA06 overexpressing native KmGUT1 and KmGUT2, URA3 recycled (5-FOA) | This study |
| **KM-G03** | KM-G01 integrated with pGLY-GDH (KpGDH), URA3 recycled (5-FOA) | This study |
| **KM-G05** | KM-G03 integrated with pGLY-DAK-MAE (KmDAK1, 2nd SpMAE1 copy), URA3 recycled | This study |
| **KM-G07** | KM-G05 integrated with 2nd copy of pSA-FRD-MAE (TbFRD/SpMAE1), URA3 recycled | This study |
| **KM-G08** | KM-G07 integrated with pGLY-FDH (KmFDH1; glycerol master chassis) | This study |

### 2.4. Shake-flask fermentations and parameter optimisation

Single colonies from fresh agar plates were inoculated into 5 mL YPD or SC-Ura in 50 mL conical tubes and grown at 37 °C and 220 rpm for 16 h. Pre-cultures in 250 mL Erlenmeyer flasks containing 50 mL YPX or YPG were inoculated at $OD_{600}$ = 0.2 and grown to mid-exponential phase ($OD_{600}$ ≈ 6.0). Cells were harvested at 4,000 × g for 5 min at 4 °C, washed twice with ice-cold sterile water and inoculated into fermentation flasks at $OD_{600}$ = 0.5 (0.16 g DCW/L). Shake-flask fermentations were conducted in 250 mL flasks containing 50 mL medium at 30, 37, 42 or 45 °C and 220 rpm for 72 h. Four process parameters were optimised sequentially on clarified SBH at 42 °C: (1) initial sugar loading (50, 100, 150 and 200 g/L total reducing sugars, supplemented with 10 g/L yeast extract and 20 g/L peptone in smooth gauze-stoppered flasks); (2) vessel geometry and aeration (smooth flask with Parafilm seal, smooth flask with eight-layer gauze stopper, baffled flask with seal, and baffled flask with eight-layer gauze stopper, at 100 g/L SBH sugars); (3) industrial nitrogen source (30 g/L soybean peptone, fish meal peptone, corn steep liquor [CSL] or cottonseed meal extract, benchmarked against 5 g/L $(NH_4)_2SO_4$ in baffled gauze-stoppered flasks at 100 g/L SBH sugars); and (4) buffering regime (unbuffered free-acid

fermentation starting at pH 5.5 with 0 g/L $CaCO_3$ against 10, 20, 30 and 40 g/L $CaCO_3$ under the optimal 100 g/L SBH sugar and 30 g/L CSL condition).

### 2.5. Bioreactor fermentations and mass-balance definitions

Bioreactor runs were performed in a 2.5 L jacketed glass stirred-tank bioreactor with an initial working volume of 1.00 L. Seed cultures grown in baffled flasks at 37 °C for 16 h were inoculated to an initial biomass concentration of $OD_{600}$ = 1.3-1.5 (0.42-0.48 g DCW/L). Temperature was controlled at 37.0 ± 0.1 °C or 42.0 ± 0.1 °C via jacket recirculation. Agitation (300–800 rpm) was cascaded to mass-flow-controlled air sparging (1.0-1.5 vvm) to maintain dissolved oxygen above 20 % of air saturation. In low-pH runs, the medium started at pH 5.5 and was allowed to self-acidify to pH 3.65 ± 0.05, where it was maintained by automated titration with 3.0 M KOH. Parallel neutral-pH benchmark runs were maintained at pH 7.0 with a 20 % (w/v) $Ca(OH)_2$ slurry to verify the downstream gypsum mass balance. No exogenous $CO_2$ enrichment was applied; metabolic $CO_2$ generated by respiration and intracellular decarboxylation supplied the dissolved inorganic carbon pool. For SBH fed-batch runs, the initial 1.00 L batch contained 60.0 g/L total sugars from clarified SBH (carrying 2.81 g/L acetic acid) and 30.0 g/L CSL. Fed-batch feeding started at 12 h when residual total sugars declined below 15 g/L. Concentrated resin-detoxified SBH feed (340.0 g/L total sugars: 265.0 g/L D-xylose, 45.0 g/L D-glucose, 25.0 g/L L-arabinose, 5.0 g/L minor sugars; 14.2 g/L acetic acid; 60.0 g/L CSL) was pumped at 8-18 mL/h from 12 to 72 h, delivering 0.510 L of feed (173.4 g sugars, 7.24 g acetic acid and 30.6 g CSL). Accounting for automated base addition (0.061 L of 3.0 M KOH = 0.183 mol KOH in the 42 °C run, matching the 0.163 mol required for partial neutralisation of 0.742 mol succinic acid at pH 3.65 plus 0.020 mol medium buffering) and cumulative sampling plus evaporative water loss (-0.071 L), the final working volume at 72 h was 1.50 L. Total sugar supplied was 233.4 g (60.0 g initial + 173.4 g fed); residual sugar at 72 h was 1.47 g/L (2.2 g in 1.50 L), giving a cumulative sugar consumption of 231.2 g (154.1 g/L normalised to final volume) and complete assimilation of the 10.05 g cumulative acetic acid supplied.

For pure glycerol and pretreated CBG fed-batch runs, the initial 1.00 L batch contained 55.0 g/L glycerol (supplied from an 800.0 g/L pure glycerol stock or the 785.0 g/L clarified CBG stock described in Section 2.2.2) with 30.0 g/L CSL. Feeding commenced at 16 h when residual glycerol fell below 15 g/L. Concentrated glycerol feed (800.0 g/L pure glycerol or 785.0 g/L clarified CBG stock co-fed with concentrated CSL/salts) was added at 3.5–9.0 mL/h between 16

and 64 h to maintain residual glycerol between 5 and 15 g/L before tapering to below 2 g/L at 72 h. In the 42 °C CBG run, 0.200 L of the 785.0 g/L clarified CBG stock (157.0 g glycerol) was fed into the 1.00 L initial batch (55.0 g glycerol), supplying 212.0 g total glycerol; with 0.070 L of 3.0 M KOH (0.210 mol KOH), 0.290 L of supplemental nutrient/water make-up and −0.060 L of sampling and evaporation, the final broth volume at 72 h was 1.50 L with 0.53 g/L (0.8 g) residual glycerol, giving 211.2 g cumulative glycerol consumed. In the 42 °C pure glycerol run, 0.207 L of 800.0 g/L glycerol feed (165.6 g glycerol) plus 55.0 g initial glycerol supplied 220.6 g total glycerol, leaving 0.53 g/L (0.8 g) residual in 1.50 L (219.8 g consumed).

Product mass yield $Y_{p/s}$ (g/g) is defined as total succinic acid mass produced divided by cumulative primary substrate mass consumed: $Y_{p/s}$ = (Pfinal · Vfinal − Pinitial · Vinitial) / Sconsumed. Volumetric productivity $Q_p$ (g/L/h) is defined as final succinic acid concentration divided by fermentation duration (24 h for 37 °C batch, 18 h for 42 °C batch, and 72 h for fed-batch runs).

### 2.6. Intracellular metabolite and cofactor quantification

Intracellular $NAD^+$ and NADH were extracted and quantified using enzymatic cycling assay kits following rapid cold-methanol quenching. Culture aliquots (10 mL) were sampled at mid-exponential phase into 20 mL of 60 % (v/v) methanol pre-chilled to -40 °C, centrifuged at 6,000 × g for 5 min at -9 °C, washed with ice-cold phosphate-buffered saline and flash-frozen in liquid nitrogen. For selective NADH determination, extracts were heated at 60 °C for 10 min to decompose $NAD^+$; $NAD^+$ was determined from acid-treated extracts. Absorbance was recorded at 450 nm on a SpectraMax iD3 plate reader. Spike-and-recovery controls gave 92.5 ± 2.8 % for NADH and 90.4 ± 3.1 % for $NAD^+$. Cofactor pools are normalised to dry cell weight (µmol/g DCW) and represent whole-cell pools without subcellular fractionation.

### 2.7. Analytical methods

Cell growth was monitored at 600 nm on a Shimadzu UV-2600 spectrophotometer and converted to dry cell weight using the calibration 1.0 $OD_{600}$ = 0.325 g DCW/L (linear range 0.05–0.80 $OD_{600}$, $R^2$ = 0.9994). D-glucose, D-xylose, L-arabinose, glycerol, succinic acid, ethanol, acetic acid, pyruvic acid and lactic acid were quantified by HPLC (Agilent 1260 Infinity II) equipped with an Aminex HPX-87H ion-exclusion column (300 × 7.8 mm; Bio-Rad) operated at 60 °C with 5 mM $H_2SO_4$ at 0.6 mL/min. Baseline separation of succinic acid (11.8 min), lactic

acid (12.8 min) and glycerol (13.6 min) was verified at chromatographic resolution $R_s > 1.8$. Succinic acid identity was confirmed by high-resolution ESI-Q-TOF LC-MS (Agilent 6545) at m/z 117.0193 ($[M-H]^-$, theoretical 117.0193). Sugars, glycerol and ethanol were detected by refractive index at 40 °C and organic acids by photodiode array at 210 nm.

### 2.8. Cooling, neutralisation and salt-generation calculations

Fermenter cooling energetics were evaluated using an explicit steady-state energy balance over a 72 h fed-batch cycle: Qcool = Qmet + Qagit − Qevap − Qsens − Qrad. For the base-case 42 °C fed-batch fermentation, specific metabolic heat generation (Qmet) computed from respiratory carbon oxidation (24.1 g C/L respired over 72 h at 38.6 kJ/g C oxidized, plus exothermic acid-formation enthalpy) averages 3.6 kW/m³; mechanical agitation power input (Qagit) for cascaded aerobic mixing (300-800 rpm, 1.0-1.5 vvm) contributes 2.8 kW/m³; and evaporative plus sensible enthalpy carried out by humidified exhaust air (Qevap + Qsens + Qrad) removes 0.4 kW/m³, yielding a net jacket cooling duty Qcool = 6.0 kW/m³ (432 kWh thermal load per tonne of broth over 72 h; sensitivity range 3.0-15.0 kW/m³ or 216-1,080 kWh/t covering low-density pentose runs to high-density aerobic yeast processes, Table S5). Cooling-tower water was modelled at a 33 °C supply temperature (28 °C ambient wet-bulb plus a 5 K tower approach) and a 5 K return range (38 °C return, specific heat capacity 4.184 kJ/kg/K = 1.162 kWh/m³/K, absorbing 5.811 kWh per m³ of water circulated). At a mesophilic broth temperature of 30 °C, cooling-tower water at 33 °C cannot cool the fermenter directly, so a mechanical vapour-compression chiller (COP = 3.8) must lift the entire 432 kWh/t jacket load, consuming 113.7 $kWh_e$ of electricity per tonne of broth and rejecting 545.7 kWh/t at the chiller condenser (93.9 m³ of tower water per tonne of broth). At 42 °C, the 9 K temperature driving force above the 33 °C tower supply allows direct jacket cooling without a chiller (0 $kWh_e$/t chiller electricity) and requires 74.3 m³/t of cooling-tower water, representing a 100 % elimination of chiller power and a 20.9 % reduction in cooling-water circulation across all heat loads. Scaled to a 1,000 m³ industrial fermenter operating 30 batches per year (30,000 t broth/year), 42 °C operation avoids 3.41 $GWh_e$/year of electricity, corresponding to 1,982 t $CO_2$-eq/year at a grid emission factor of 0.581 kg $CO_2/kWh_e$ (Table S5).

Neutralisation stoichiometry and downstream salt generation were calculated from the Henderson–Hasselbalch speciation of diprotic succinic acid ($pKa_1$ = 4.21, $pKa_2$ = 5.64). At pH 3.65, the undissociated free acid ($H_2Suc$), monoanion ($HSuc^-$) and dianion ($Suc^{2-}$) mole fractions are 78.23 %, 21.55 % and 0.22 %, requiring 0.220 mol of hydroxide equivalents per mol of

succinic acid produced (0.2155 + 2 × 0.0022). By contrast, at pH 7.0 the speciation is 0.01 % $H_2Suc$, 4.18 % $HSuc^-$ and 95.81 % $Suc^{2-}$, requiring 1.958 mol $OH^-$ equivalents (0.979 mol $Ca(OH)_2$) per mol of succinic acid, and subsequent acidification with $H_2SO_4$ precipitates 1,458 kg of insoluble $CaSO_4 \cdot 2H_2O$ (gypsum) sludge per tonne of succinic acid recovered (or 320.6 kg/t if $Ca(OH)_2$ were used at pH 3.65). Because the present process operates at pH 3.65 with KOH titration, calcium is completely absent from the fermentation and recovery train: solid gypsum generation is 0 kg/t, and both base demand during fermentation and $H_2SO_4$ demand during downstream crystallisation acidification are reduced by 78.0 % relative to neutral-pH operation. Neutralising the 0.220 eq/mol potassium succinate fraction with $H_2SO_4$ during downstream direct-crystallisation recovery generates 0.110 mol $K_2SO_4$ per mol succinic acid (162 kg soluble $K_2SO_4$ per tonne of succinic acid theoretically, or 224 kg/t including medium buffering), which remains in the aqueous mother liquor and can be recovered as chloride-free potassium sulfate fertiliser or regenerated via bipolar membrane electrodialysis rather than disposed of as gypsum landfill waste.

### 2.9. Carbon balance

Carbon balances were closed for the shake-flask knockout series (Table 2) and for the 42 °C fed-batch bioreactor runs on SBH, pure glycerol and CBG (Table S4). For SBH fermentations, total quantifiable substrate carbon was calculated as the sum of measured sugar carbon consumed (0.400 g C per g sugar mixture) and initial/fed hydrolysate acetic acid carbon supplied (0.400 g C per g acetic acid); for glycerol fermentations, substrate carbon was taken as 0.391 g C per g glycerol consumed. Quantified extracellular product carbon was summed from the measured concentrations of succinic acid (0.407 g C/g), ethanol (0.521 g C/g), glycerol (0.391 g C/g), residual broth acetic acid (0.400 g C/g) and pyruvic acid (0.409 g C/g). Biomass carbon was calculated using a standard elemental composition of 0.470 g C per g DCW. Because off-gas $CO_2$ was not measured online and complex nitrogen supplements (yeast extract/peptone or CSL) also contribute assimilable amino-acid carbon for biomass synthesis, the $CO_2$ + unmeasured term is reported explicitly as a mass-balance closure term rather than a direct gas-phase measurement.

## 3. Results

### 3.1. Construction of the reductive TCA pathway in K. marxianus

To establish reductive succinic acid biosynthesis in K. marxianus, a cytosolic rTCA conduit was assembled on top of a xylose-assimilating chassis (Fig. 1A). SpCas9 was first

integrated at the fcy1 locus of KM-01U to generate KM-Cas9. For D-xylose assimilation without cofactor imbalance, codon-optimised AcXI and native KmXKS1 were integrated (KM-X01), followed by overexpression of the non-oxidative pentose phosphate pathway enzymes KmTAL1 and KmTKL1 to yield KM-X02 (Table 1). The rTCA module was then introduced by sequential integration of pSA-rTCA (AsPCK under PKmTDH3 and CgMDH under PKmPGK1) and pSA-FRD-MAE (TbFRD under PKmGAP and SpMAE1 under PKmENO1) along with native fumarase (KmFUM1), yielding KM-SA01 and its URA3-cured derivative KM-SA02 (Table 1). KM-SA01 was evaluated in shake flasks at 30, 37 and 42 °C on 50 g/L D-glucose, D-xylose and clarified SBH (Fig. 1B–D). Whereas wild-type KM-WT accumulated no detectable extracellular succinic acid, KM-SA01 produced succinic acid across all three substrates and temperatures: 1.85 ± 0.09, 1.68 ± 0.08 and 1.52 ± 0.07 g/L at 30 °C (Fig. 1B); 2.42 ± 0.11, 2.25 ± 0.10 and 2.10 ± 0.09 g/L at 37 °C (Fig. 1C); and 2.84 ± 0.13, 2.65 ± 0.12 and 2.51 ± 0.11 g/L at 42 °C (Fig. 1D) on glucose, xylose and SBH, respectively. The positive temperature dependence reflects the native thermotolerance of *K. marxianus* and the high thermal optimum of A. cellulolyticus xylose isomerase.

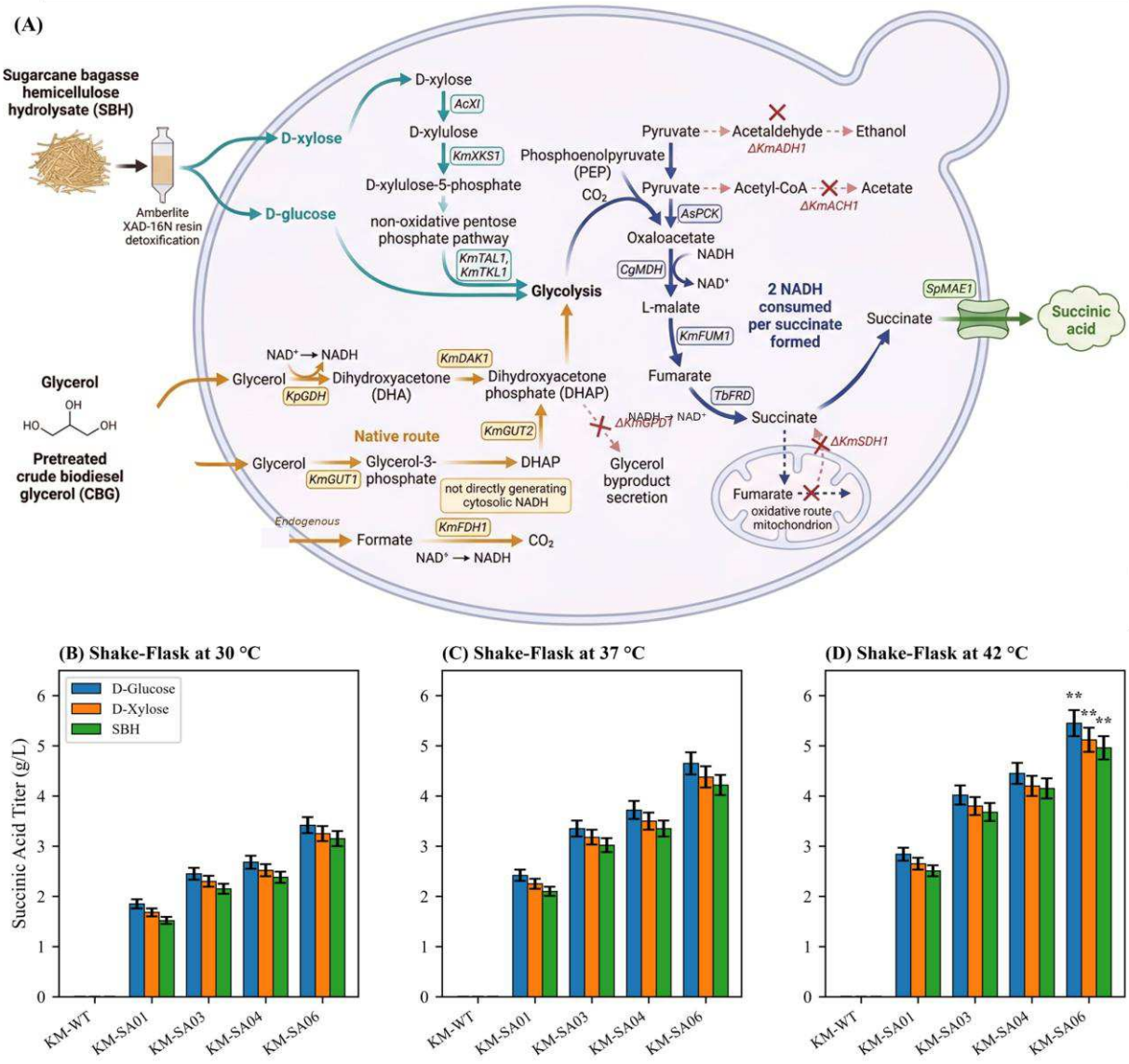



**Fig. 1** (A) Engineered metabolic network in *Kluyveromyces marxianus* for succinic acid biosynthesis from sugarcane bagasse hemicellulose hydrolysate (SBH) and pretreated crude biodiesel glycerol (CBG). Solid blue arrows denote the engineered cytosolic rTCA conduit (AsPCKcarboxylating PEP to oxaloacetate, CgMDH, KmFUM1, NADH-dependent TbFRD and the dicarboxylate exporter SpMAE1); red crosses mark the four CRISPR/Cas9-deleted competing reactions (ΔKmADH1, ΔKmGPD1, ΔKmSDH1 and ΔKmACH1). (B–D) Succinic acid titres of KM-WT, KM-SA01, KM-SA03, KM-SA04 and KM-SA06 in shake flasks on D-glucose, D-xylose and clarified SBH (50 g/L initial sugars, 72 h) at 30 °C (B), 37 °C (C) and 42 °C (D). Values are mean ± SD of biological triplicates (n = 3); asterisks denote statistical significance relative to KM-SA01 (**p < 0.01, one-way ANOVA with Tukey's HSD test)

### 3.2. Elimination of competing carbon sinks and byproduct pathways

During shake-flask fermentation of KM-SA01 on clarified SBH (50.0 g/L initial sugars, carrying 2.34 g/L initial acetic acid; 42 °C, 72 h), four soluble byproducts accumulated to a combined broth concentration of 28.44 ± 1.00 g/L: ethanol (18.42 ± 0.75 g/L), glycerol (4.85 ± 0.22 g/L), broth acetic acid (3.92 ± 0.18 g/L, representing 1.58 g/L net acetate excretion above the 2.34 g/L supplied in SBH) and pyruvic acid (1.25 ± 0.08 g/L). Succinic acid reached only 2.51 ± 0.11 g/L (yield 0.050 ± 0.002 g/g sugar), representing 7.0 % C-mol of total quantified extracellular products (or 7.5 % of net de novo excreted product carbon), alongside 5.42 ± 0.21 g DCW/L of final biomass (Fig. 2A–D). Because these competing reactions divert pyruvate, DHAP and PEP away from the rTCA conduit and re-oxidise cytosolic NADH, four sequential CRISPR/Cas9 disruptions were introduced (Fig. 1A, Fig. 2A–D). (1) Disrupting KmADH1 in KM-SA03 reduced ethanol accumulation by 95.4 % (from 18.42 to 0.85 ± 0.06 g/L; $p = 1.8 \times 10^{-13}$), raising the succinic acid titre by 46.6 % to 3.68 ± 0.18 g/L ($p = 1.7 \times 10^{-4}$) and final biomass to 6.85 ± 0.25 g DCW/L, while partially redirecting NADH re-oxidation into glycerol (5.12 ± 0.24 g/L) and pyruvic acid (1.42 ± 0.09 g/L). (2) Deleting KmGPD1 in KM-SA04 curtailed glycerol secretion by 88.7 % (to 0.55 ± 0.04 g/L; $p = 6.0 \times 10^{-11}$) and elevated succinic acid to 4.15 ± 0.20 g/L (+65.3 % over KM-SA01; $p = 8.4 \times 10^{-6}$), with pyruvic acid peaking at 1.55 ± 0.08 g/L and product-carbon selectivity reaching 39.7 % C-mol. (3) Disrupting KmSDH1 in KM-SA05 prevented mitochondrial oxidation of succinate to fumarate, increasing the succinic acid titre to 4.62 ± 0.22 g/L (+84.1 %; $p = 7.9 \times 10^{-7}$) and lowering pyruvic acid to 1.10 ± 0.06 g/L, with a modest reduction in 72 h biomass (7.12 ± 0.26 vs 7.48 ± 0.27 g DCW/L in KM-SA04). (4) Deleting KmACH1 in KM-SA06 eliminated mitochondrial acetyl-CoA hydrolysis to free acetate, increasing 72 h biomass to 8.95 ± 0.31 g DCW/L and lowering total residual soluble byproducts to 2.53 ± 0.07 g/L (0.65 ± 0.04 g/L ethanol, 0.48 ± 0.03 g/L glycerol, 0.28 ± 0.03 g/L residual acetic acid and 1.12 ± 0.06 g/L pyruvic acid) a 91.1 % reduction in total byproduct concentration. At 42 °C, KM-SA06 produced 5.45 ± 0.26 g/L succinic acid on glucose, 5.12 ± 0.24 g/L on xylose and 4.96 ± 0.23 g/L on clarified SBH (yield 0.099 ± 0.005 g/g sugar), representing a 97.6 % increase in titre over KM-SA01 ($p = 1.9 \times 10^{-7}$) and a 9.2-fold increase in product-carbon selectivity from 7.0 to 64.3 % C-mol of total quantified extracellular products (Fig. 2C).

The acetate balance across the knockout series highlights a metabolic transition from net excretion to net assimilation. Diluted to 50.0 g/L total sugars, the clarified SBH medium

introduces 2.34 g/L of exogenous acetic acid (0.94 g C/L). Whereas KM-SA01–KM-SA05 ended with 3.65–3.92 g/L of broth acetic acid (corresponding to net excretion of 1.31–1.58 g/L), KM-SA06 left only 0.28 ± 0.03 g/L of residual acetate in the broth (−92.9 % relative to KM-SA01), corresponding to a net uptake of 2.06 g/L (0.82 g C/L) of feedstock acetate via native acetyl-CoA synthetase (KmACS1/2) into the tricarboxylic acid and glyoxylate/biomass pools once futility through KmACH1 was blocked. Similarly, the carbon fate of blocked ethanolic fermentation is resolved by Table 2: in the single ΔKmadh1 step (KM-SA01 → KM-SA03), removing 9.16 g C/L of ethanol carbon (9.60 to 0.44 g C/L) increased succinate carbon by 0.48 g C/L (1.02 to 1.50 g C/L) and biomass carbon by 0.67 g C/L (2.55 to 3.22 g C/L), while respiratory $CO_2$ carbon increased by 7.98 g C/L (from 3.79 to 11.77 g C/L). Across the complete four-knockout progression (KM-SA01 → KM-SA06), succinate carbon increased by 1.00 g C/L (1.02 to 2.02 g C/L), biomass carbon increased by 1.66 g C/L (2.55 to 4.21 g C/L), total byproduct carbon fell by 12.46 g C/L (13.58 to 1.12 g C/L), and respiratory $CO_2$ closure carbon rose by 9.80 g C/L (3.79 to 13.59 g C/L). Thus, in an Crabtree-negative respiratory yeast at pH 3.65, abolishing fermentative overflow channels most of the liberated pyruvate flux through mitochondrial respiration, identifying respiratory competition and dissolved $CO_2$ availability for PEP carboxylation as the primary remaining yield constraints.

### 3.2.1. Carbon balance of the knockout series

Complete carbon balances for KM-SA01 through KM-SA06 are presented in Table 2, accounting explicitly for both the 20.00 g C/L of SBH sugars (50.0 g/L × 0.400 g C/g) and the 0.94 g C/L of exogenous acetic acid carried in with the hydrolysate (2.34 g/L × 0.400 g C/g; total quantifiable substrate carbon = 20.94 g C/L). Table 2 reports both gross final broth byproduct carbon and net de novo acetate carbon flux (+0.63 g C/L excreted in KM-SA01 vs −0.82 g C/L assimilated in KM-SA06). Across the series, total extracellular product carbon contracted from 14.60 to 3.14 g C/L while succinate's share of quantified extracellular product carbon rose from 7.0 to 64.3 % C-mol (and from 7.5 to 66.9 % C-mol on a net non-acetate byproduct basis).

**Table 2. Reconciled carbon balance of the knockout series on clarified SBH (50.0 g/L sugars + 2.34 g/L initial acetate = 20.94 g C/L total substrate carbon; 42 °C, 72 h).**

| Strain | Input C[a] (g C/L) | Succinate C (g C/L) | Gross Byp. C[b] (g C/L) | Net Acet. Flux[c] (g C/L) | Biomass C[d] (g C/L) | $CO_2$ Closure C[e] (g C/L) | Succinate Share[f] (% C-mol) |
|---|---|---|---|---|---|---|---|
| **KM-SA01** | 20.94 | 1.02 | 13.58 | +0.63 | 2.55 | 3.79 | 7.0 % (7.5 %) |
| **KM-SA03** | 20.94 | 1.50 | 4.45 | +0.58 | 3.22 | 11.77 | 25.2 % (27.6 %) |
| **KM-SA04** | 20.94 | 1.69 | 2.56 | +0.56 | 3.52 | 13.17 | 39.7 % (45.1 %) |
| **KM-SA05** | 20.94 | 1.88 | 2.42 | +0.52 | 3.35 | 13.29 | 43.7 % (49.0 %) |
| **KM-SA06** | 20.94 | 2.02 | 1.12 | −0.82 | 4.21 | 13.59 | 64.3 % (66.9 %) |

[a] Input C = 20.00 g C/L from SBH sugars (50.0 g/L × 0.400 g C/g) + 0.94 g C/L from initial SBH acetic acid (2.34 g/L × 0.400 g C/g). [b] Gross Byp. C sums final broth ethanol, glycerol, pyruvic acid and residual broth acetic acid (1.57, 1.52, 1.50, 1.46 and 0.11 g C/L across KM-SA01 to KM-SA06). [c] Net Acet. Flux = final broth acetate C minus 0.94 g C/L initial SBH acetate C (negative value in KM-SA06 denotes net uptake of 2.06 g/L acetate). [d] Biomass C = 72 h dry cell weight (5.42, 6.85, 7.48, 7.12 and 8.95 g DCW/L) × 0.470 g C/g DCW. [e] $CO_2$ Closure C = Input C (20.94) − Succinate C − Gross Byp. C − Biomass C (identical to Sugar C [20.00] − Succinate C − Net Byp. C − Biomass C); obtained by difference. [f] Succinate share of total quantified extracellular product C (Succinate C / [Succinate C + Gross Byp. C]); parenthetical value excludes exogenous acetate.

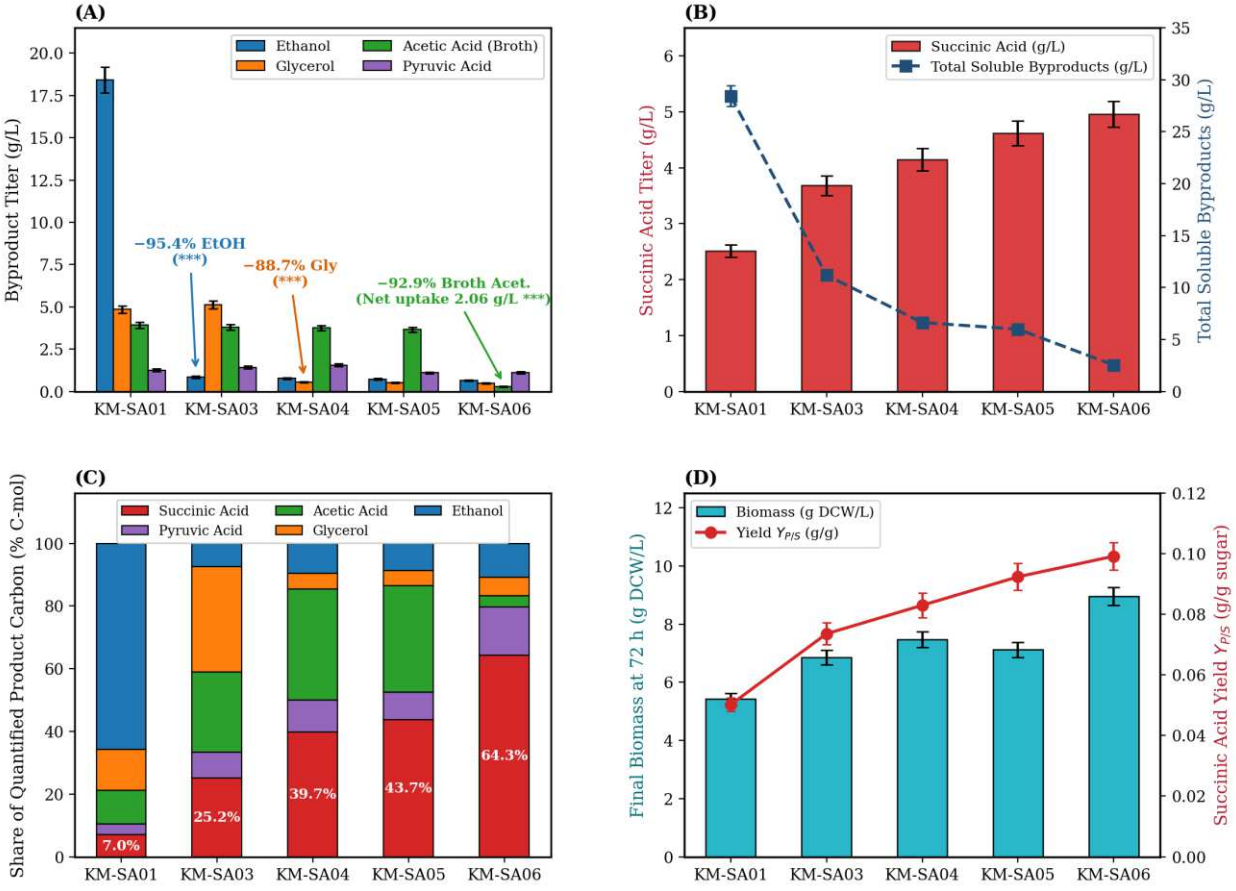



**Fig. 2** Stepwise elimination of competing carbon sinks in *K. marxianus* on clarified SBH (50.0 g/L initial sugars, 2.34 g/L initial acetic acid, 42 °C, 72 h). (A) Individual final broth byproduct titres across KM-SA01 and the sequential knockouts KM-SA03 (ΔKmadh1), KM-SA04 (+ΔKmgpd1), KM-SA05 (+ΔKmsdh1) and KM-SA06 (+ΔKmach1). (B) Succinic acid titre (bars, left axis) against total residual soluble byproducts (dashed line, right axis). (C) Extracellular soluble metabolite carbon partitioning (% C-mol of quantified broth products, matching Table 2). (D) Final biomass at 72 h (bars, left axis) and succinic acid mass yield on sugar (line, right axis). Values are mean ± SD (n = 3)

### 3.3. Growth dynamics and fermentation kinetics

KM-SA06 growth and fermentation kinetics were characterised in shake flasks on clarified SBH (50 g/L initial sugars) at 30, 37, 42 and 45 °C over 72 h (Fig. 3A–D). At 30 °C, the maximum specific growth rate ($\mu_{max}$) was 0.31 ± 0.015 $h^{-1}$, biomass reached 7.15 ± 0.28 g DCW/L ($OD_{600}$ = 22.0) at 48 h, and sugars were exhausted by 60 h to yield 3.15 ± 0.15 g/L of succinic acid (Fig. 3A). At 37 °C, $\mu_{max}$ rose to 0.46 ± 0.021 $h^{-1}$, sugars were depleted within 44 h, biomass peaked at 8.25 ± 0.32 g DCW/L at 40 h (8.05 ± 0.30 g DCW/L at 72 h), and the succinic acid titre reached 4.22 ± 0.20 g/L (Fig. 3B). At 42 °C, $\mu_{max}$ reached 0.58 ± 0.025 $h^{-1}$ (87.1 % higher than at 30 °C), the 50 g/L sugar load was consumed within 28 h, and biomass reached 8.95 ± 0.35 g DCW/L at 32 h (8.65–8.95 g DCW/L across 32–72 h) with a final succinic acid titre of 4.96 ± 0.23 g/L (Fig. 3C). At 45 °C, growth slowed ($\mu_{max}$ = 0.44 ± 0.019 $h^{-1}$) but KM-SA06 still accumulated 4.18 ± 0.19 g/L succinic acid. The instantaneous peak specific succinic acid production rate ($q_p$, evaluated over the steepest 8–20 h production window) increased from 0.042 ± 0.003 g/g DCW/h at 30 °C to 0.076 ± 0.005 g/g DCW/h at 37 °C and 0.112 ± 0.007 g/g DCW/h at 42 °C (Fig. 3D). Initial rapid growth at 42 °C reflects consumption of the D-glucose fraction during the first 8 h, followed by steady conversion of the D-xylose-rich remainder.

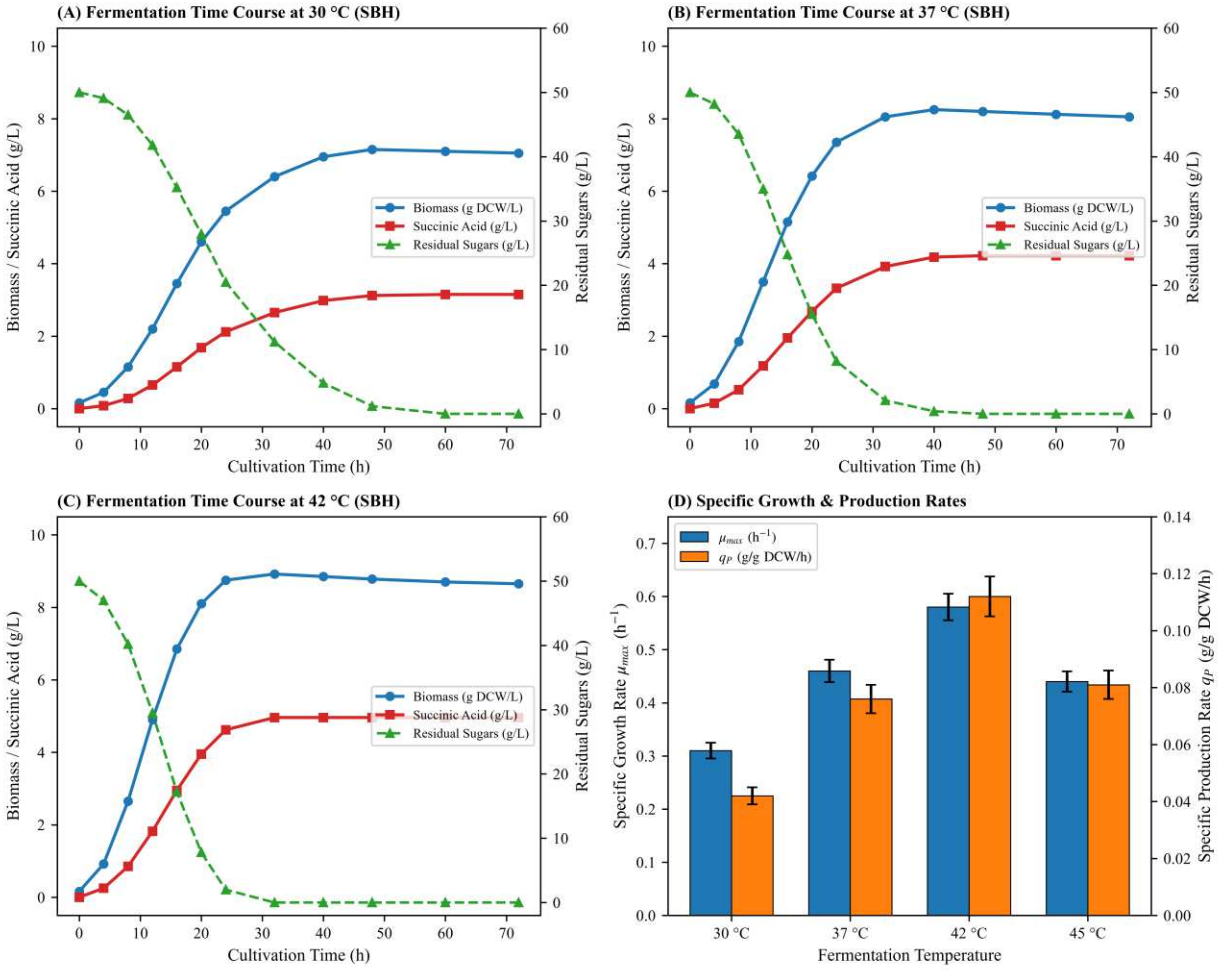



**Fig. 3** Fermentation kinetics of KM-SA06 on sugarcane bagasse hemicellulose hydrolysate (50 g/L initial sugars) in shake flasks. Time courses of biomass (g DCW/L), residual total sugars (g/L) and succinic acid (g/L) at 30 °C (A), 37 °C (B) and 42 °C (C). (D) Maximum specific growth rate ($\mu_{max}$, $h^{-1}$) and peak specific succinic acid production rate ($q_p$, g/g DCW/h) across 30, 37, 42 and 45 °C. Values are mean ± SD (n = 3)

### 3.4. Fermentation engineering and parameter optimisation on SBH

Four shake-flask process parameters were optimised sequentially at 42 °C for KM-SA06 on clarified SBH (Fig. 4A–D). (1) Initial substrate loading (Fig. 4A): increasing initial SBH sugars from 50 to 100 g/L raised the succinic acid titre from 4.96 ± 0.23 to 10.42 ± 0.48 g/L from 97.2 g/L sugar consumed (yield 0.107 g/g). Further increases to 150 and 200 g/L induced osmotic and residual inhibitor stress, reducing the yield to 0.083 g/g (11.05 ± 0.51 g/L) and 0.068 g/g (9.85 ± 0.44 g/L); 100 g/L initial sugar was therefore selected. (2) Vessel geometry and aeration (Fig. 4B): baffled flasks with eight-layer gauze stoppers supported 8.85 ± 0.35 g DCW/L biomass and 11.15 ± 0.52 g/L succinic acid, outperforming sealed smooth flasks (3.12 ± 0.16 g/L), gauze smooth flasks (7.25 ± 0.34 g/L) and sealed baffled flasks (6.85 ± 0.31 g/L) because ATP-generating oxidative phosphorylation is required to sustain growth and gluconeogenic/anaplerotic maintenance at low pH. (3) Industrial nitrogen source (Fig. 4C): replacing refined peptone/yeast extract with 30 g/L corn steep liquor (CSL) in unbuffered baffled gauze flasks raised the succinic acid titre to 12.86 ± 0.58 g/L (yield 0.132 g/g), surpassing cottonseed meal (10.15 ± 0.46 g/L), soybean peptone (9.24 ± 0.42 g/L), fish meal peptone (8.45 ± 0.39 g/L) and the inorganic $(NH_4)_2SO_4$ control (6.82 ± 0.31 g/L). (4) Buffering regime (Fig. 4D): in the unbuffered free-acid control (0 g/L $CaCO_3$, 100 g/L SBH sugars, 30 g/L CSL), accumulation of 12.86 ± 0.58 g/L (109 mM) succinic acid drove the final broth pH down from 5.50 to 2.95 ± 0.06 (well below succinic acid $pKa_1$ = 4.21). Supplementing 10, 20, 30 and 40 g/L $CaCO_3$ buffered the final broth pH at 4.15, 5.10, 5.85 and 6.18 and raised the succinic acid titre to 14.85 ± 0.65, 16.60 ± 0.72, 17.82 ± 0.75 and 17.95 ± 0.78 g/L, respectively. Thus, unbuffered acidification to pH 2.95 in shake flasks imposes a 27.8 % titre penalty relative to $CaCO_3$ buffering at pH 5.85 (12.86 vs 17.82 g/L), motivating active pH-stat control at pH 3.65 in stirred-tank bioreactors.

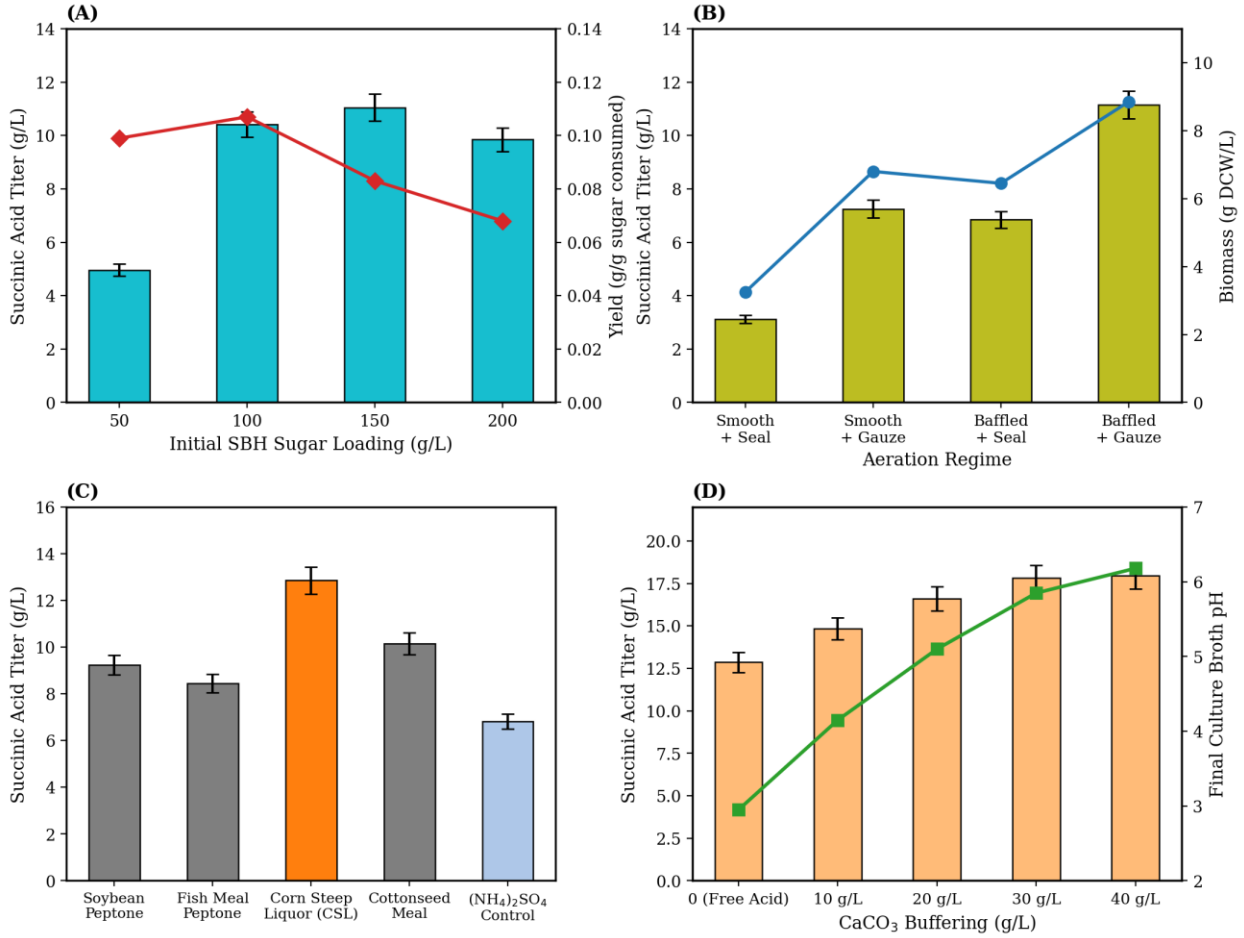



**Fig. 4** Process parameter optimisation for KM-SA06 on sugarcane bagasse hemicellulose hydrolysate at 42 °C in shake flasks (72 h). (A) Initial SBH sugar loading (50–200 g/L) showing succinic acid titre (bars) and mass yield (diamonds). (B) Aeration and vessel geometry at 100 g/L SBH sugars: smooth flask + seal, smooth flask + gauze, baffled flask + seal, and baffled flask + gauze. (C) Industrial nitrogen sources (30 g/L) against 5 g/L $(NH_4)_2SO_4$ control in unbuffered baffled gauze flasks. (D) Unbuffered free-acid fermentation (0 g/L $CaCO_3$, matching the 12.86 ± 0.58 g/L CSL condition in panel C and ending at pH 2.95) against $CaCO_3$ buffering (10–40 g/L), with final broth pH (squares, right axis). Values are mean ± SD (n = 3)

### 3.5. Scale-up to 2.5 L bioreactors on bagasse hydrolysate

KM-SA06 was scaled up to a 2.5 L stirred-tank bioreactor on clarified SBH with dissolved oxygen maintained above 20 % saturation and broth pH controlled at 3.65 ± 0.05 by automated titration with 3.0 M KOH (Fig. 5A–D). In batch mode with 60.0 g/L initial SBH sugars at 37 °C (Fig. 5A), sugars were consumed within 24 h, biomass reached 10.5 ± 0.4 g DCW/L, and succinic acid reached 19.65 ± 0.82 g/L, corresponding to a yield of 0.328 g/g sugar and a batch volumetric productivity of 0.819 g/L/h. At 42 °C (Fig. 5B), batch sugar depletion accelerated to 18 h, biomass reached 12.1 ± 0.5 g DCW/L, and succinic acid reached 23.50 ± 0.95 g/L, giving a mass yield of 0.392 g/g sugar and a batch productivity of 1.306 g/L/h (59.5 % higher productivity than at 37 °C). In fed-batch mode supplied with concentrated resin-detoxified SBH (340.0 g/L sugars) over 72 h, the 37 °C culture (Fig. 5C) reached 26.8 ± 0.9 g DCW/L biomass and 48.25 ± 1.85 g/L succinic acid (72.38 g in 1.50 L final volume) from 218.5 g consumed sugar, corresponding to a cumulative yield of 0.331 g/g and an overall productivity of 0.670 g/L/h. At 42 °C (Fig. 5D), fed-batch biomass reached 29.4 ± 1.0 g DCW/L and succinic acid reached 58.42 ± 2.15 g/L (87.63 g in 1.50 L) from 231.2 g consumed sugar, achieving a cumulative yield of 0.379 ± 0.014 g/g sugar (33.7 % of the 1.124 g/g redox-balanced sugar ceiling) and an overall volumetric productivity of 0.811 g/L/h. Closing the fed-batch carbon balance on total quantifiable substrate carbon (92.48 g sugar C + 4.02 g assimilated feed acetate C = 96.50 g C; Table S4) accounts for 35.65 g C (36.9 %) in succinic acid, 20.73 g C (21.5 %) in biomass and 40.12 g C (41.6 %) in respired $CO_2$ closure (or 38.6 %, 22.4 % and 39.0 % normalised to the 92.48 g sugar carbon input alone). The 2.9-fold increase in yield from unbuffered CSL shake flasks (0.132 g/g, ending at pH 2.95) to the pH-stat bioreactor (0.379–0.392 g/g, held at pH 3.65 with controlled DO > 20 %) directly reflects the prevention of extreme acidification below pH 3.0 which otherwise collapses the plasma-membrane proton-motive force and consumes ATP via $H^+$-ATPase proton extrusion together with improved gas–liquid mass transfer.

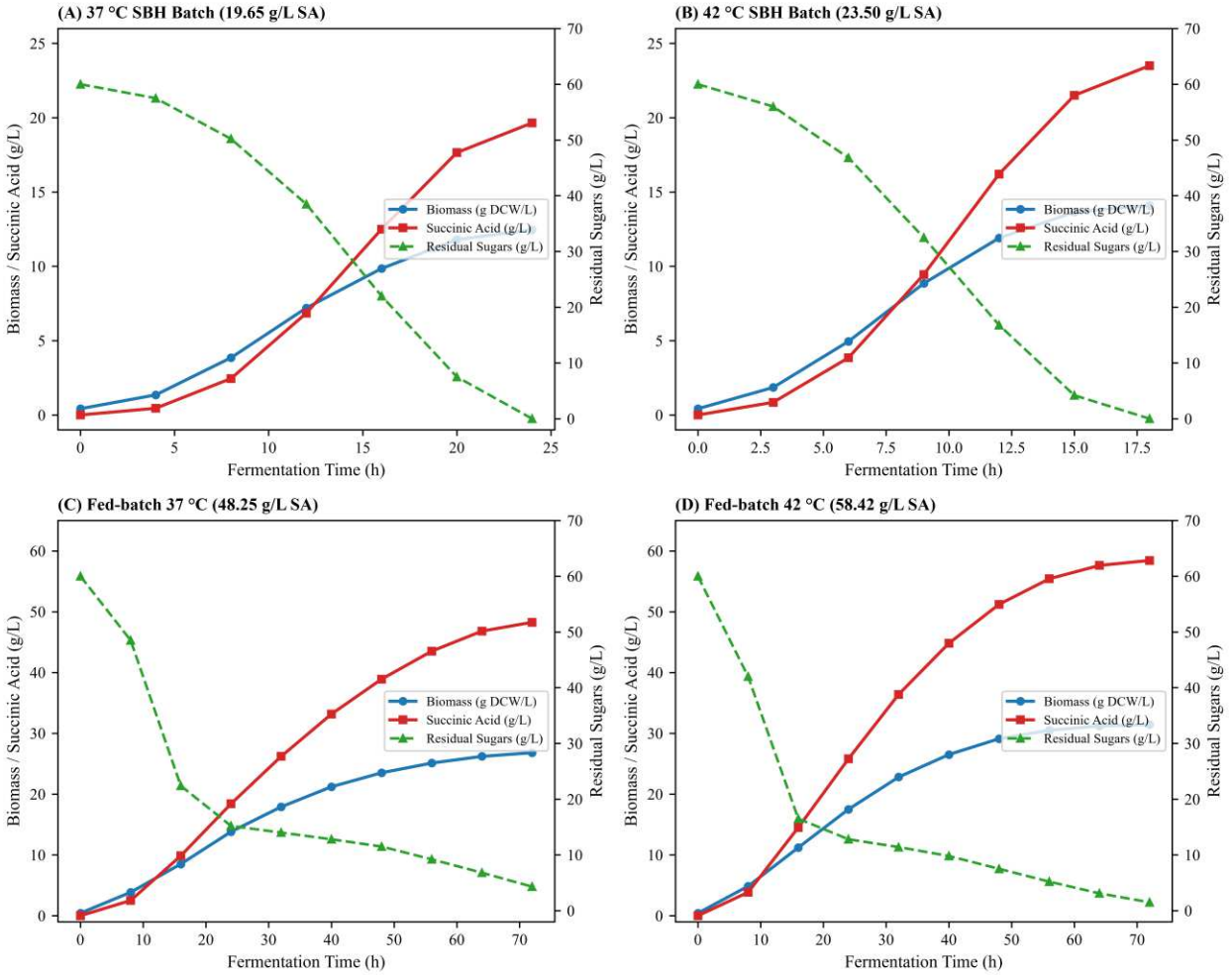


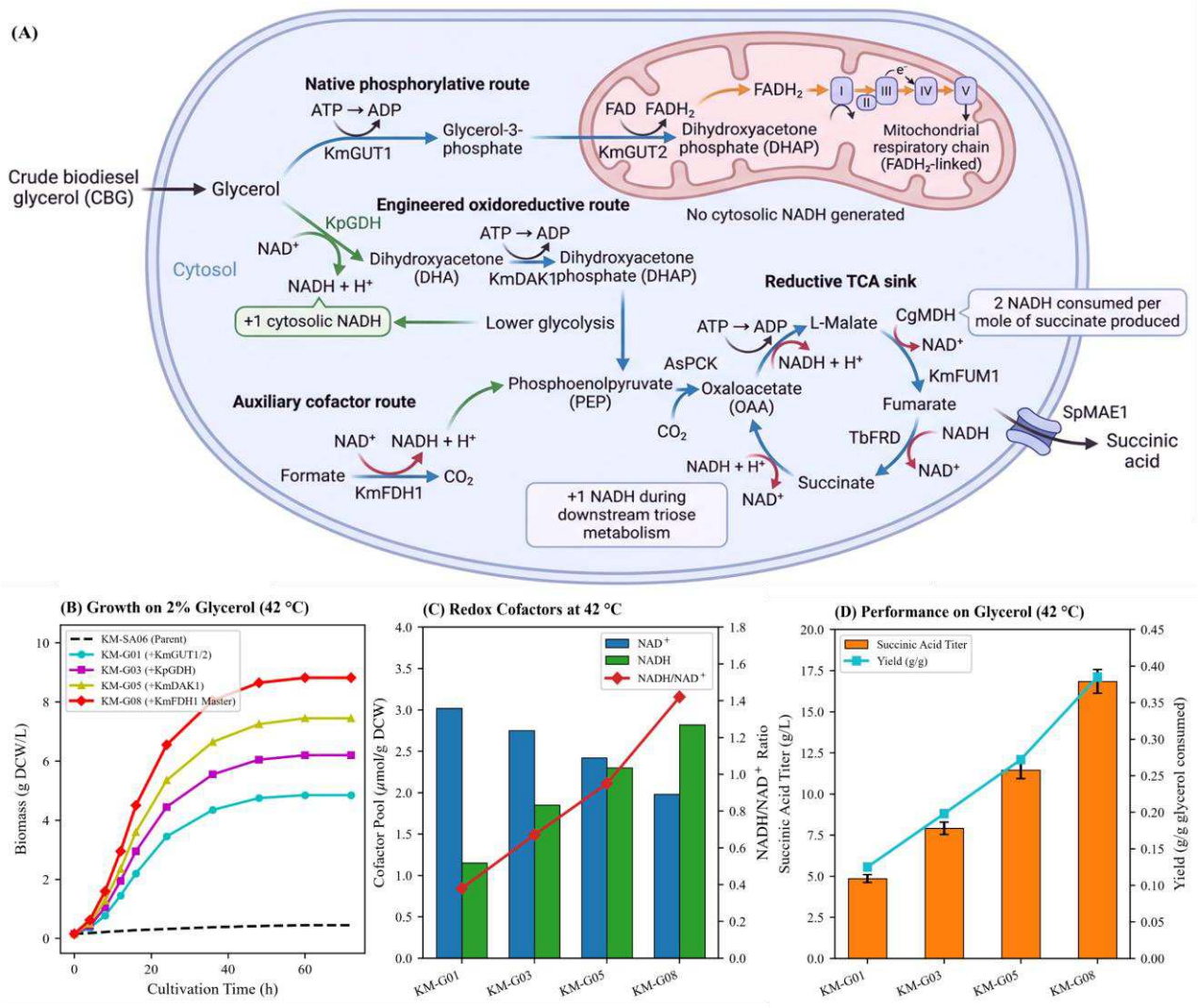

**Fig. 5** Scale-up of KM-SA06 on sugarcane bagasse hemicellulose hydrolysate in a 2.5 L stirred-tank bioreactor at pH 3.65 (titrated with 3.0 M KOH). (A) Batch fermentation at 37 °C (19.65 g/L, 24 h). (B) Batch fermentation at 42 °C (23.50 g/L, 18 h). (C) Fed-batch fermentation at 37 °C with concentrated SBH feed (48.25 g/L, 72 h). (D) Fed-batch fermentation at 42 °C with concentrated SBH feed (58.42 g/L, 72 h). Profiles show biomass (g DCW/L), residual total sugars (g/L) and succinic acid (g/L). Values are mean ± SD (n = 3)

### 3.6. Glycerol valorisation and NADH cofactor engineering

To extend the substrate range to biodiesel co-products and overcome the cytosolic NADH limitation inherent to sugar catabolism, KM-SA06 was engineered for oxidoreductive glycerol assimilation (Fig. 6A). (1) Wild-type *K. marxianus* assimilates glycerol poorly via glycerol kinase (KmGUT1) and mitochondrial FAD-dependent glycerol-3-phosphate dehydrogenase (KmGUT2), which transfers electrons directly to ubiquinone ($FADH_2$) in the respiratory chain without generating cytosolic NADH (Cui et al. 2017; Gao et al. 2016). Overexpressing native KmGUT1 and KmGUT2 in KM-SA06 (giving KM-G01) increased 60 h biomass on 20 g/L glycerol at 42 °C from 0.45 ± 0.05 g DCW/L in KM-SA06 to 4.80 ± 0.21 g DCW/L (a 10.7-fold increase; Fig. 6B). (2) Introducing heterologous $NAD^+$-dependent glycerol dehydrogenase from *K. pneumoniae* (KpGDH, strain KM-G03) established oxidation of glycerol to dihydroxyacetone (DHA) coupled to 1 mol of cytosolic NADH generation, lifting biomass by 29.2 % to 6.20 ± 0.24 g DCW/L. (3) Overexpressing native dihydroxyacetone kinase (KmDAK1, which phosphorylates DHA to DHAP using ATP) together with a second copy of the exporter SpMAE1 (strain KM-G05) routed flux into lower glycolysis where conversion of DHAP/GAP to PEP via glyceraldehyde-3-phosphate dehydrogenase yields a second mole of cytosolic NADH per mole of glycerol and raised biomass to 7.40 ± 0.28 g DCW/L (+19.4 %). (4) Integrating a second copy of the TbFRD-SpMAE1 cassette (KM-G07) followed by native $NAD^+$-dependent formate dehydrogenase yielded the glycerol master chassis, reaching 8.82 ± 0.38 g DCW/L biomass at 60 h (a 19.6-fold increase over KM-SA06; Fig. 6B).

Whole-cell pyridine nucleotide measurements confirmed a progressive shift toward a more reduced intracellular state across the glycerol engineering series (Fig. 6C). Whole-cell NADH rose from 1.15 ± 0.06 µmol/g DCW in KM-G01 ($NADH/NAD^+$ ratio = 0.38 ± 0.02) to 1.85 ± 0.09 µmol/g DCW in KM-G03 (ratio = 0.67 ± 0.03), 2.30 ± 0.11 µmol/g DCW in KM-G05 (ratio = 0.95 ± 0.05) and 2.82 ± 0.14 µmol/g DCW in KM-G08 (ratio = 1.42 ± 0.07), representing a 145.2 % expansion of the intracellular NADH pool. Driven by this elevated reducing power and amplified rTCA sink, KM-G08 produced 16.85 ± 0.72 g/L succinic acid in shake flasks on 50 g/L pure glycerol at 42 °C from 43.8 g/L glycerol consumed (yield 0.385 ± 0.016 g/g), a 247.4 % increase over KM-G01 (4.85 ± 0.22 g/L, yield 0.125 g/g; Fig. 6D). Because KM-G08 combines both rTCA sink amplification (via the second TbFRD/SpMAE1 copy in KM-G07) and KmFDH1 overexpression without exogenous formate addition, the primary stoichiometric NADH driver is

the coupled KpGDH → KmDAK1 → lower-glycolysis (GAPDH) sequence which generates exactly 2 mol cytosolic NADH per mol glycerol converted to PEP while KmFDH1 acts only on




trace endogenous formate derived from one-carbon/folate turnover.

**Fig. 6** Glycerol valorisation and NADH cofactor engineering in K. marxianus. (A) Native phosphorylative glycerol pathway (KmGUT1/KmGUT2, $FADH_2$-linked), engineered oxidoreductive pathway (KpGDH generating 1 NADH at glycerol → DHA, KmDAK1 phosphorylating DHA → DHAP, and lower glycolysis generating a second NADH at GAPDH), auxiliary endogenous formate oxidation (KmFDH1) and NADH coupling to the rTCA sink (2 NADH consumed per succinate). (B) Growth profiles on 20 g/L glycerol at 42 °C. (C) Whole-cell $NAD^+$ and NADH pools (μmol/g DCW) and NADH/$NAD^+$ ratio across KM-G01, KM-G03, KM-

G05 and KM-G08 at 42 °C. (D) Succinic acid titre (bars) and mass yield (line) on 50 g/L glycerol in shake flasks at 42 °C. Values are mean ± SD (n = 3)

### 3.7. Fed-batch fermentation on pure and crude biodiesel glycerol

KM-G08 was evaluated in 2.5 L fed-batch bioreactors at pH 3.65 (titrated with 3.0 M KOH) on pure glycerol and on the clarified 785.0 g/L CBG feed stock at 37 and 42 °C (Fig. 7A–D). On pure glycerol at 37 °C (Fig. 7A), biomass reached 28.5 ± 0.9 g DCW/L and 56.40 ± 2.10 g/L succinic acid accumulated over 72 h (84.60 g in 1.50 L) from 198.5 g consumed glycerol, giving a cumulative yield of 0.426 ± 0.016 g/g and a volumetric productivity of 0.783 g/L/h. At 42 °C on pure glycerol (Fig. 7B), biomass reached 33.5 ± 1.1 g DCW/L and the succinic acid titre reached 71.20 ± 2.65 g/L (106.80 g in 1.50 L) from 219.8 g consumed glycerol (55.0 g initial + 165.6 g fed in 0.207 L of 800 g/L feed, minus 0.8 g residual), corresponding to a cumulative yield of 0.486 ± 0.018 g/g and a volumetric productivity of 0.989 g/L/h. On clarified CBG at 37 °C (Fig. 7C), biomass reached 25.2 ± 0.8 g DCW/L and succinic acid reached 51.85 ± 1.95 g/L (77.78 g in 1.50 L) from 188.2 g consumed glycerol (yield 0.413 ± 0.015 g/g; productivity 0.720 g/L/h). At 42 °C on clarified CBG (Fig. 7D), biomass reached 31.4 ± 1.0 g DCW/L and succinic acid reached 65.18 ± 2.40 g/L (97.77 g in 1.50 L) from 211.2 g consumed glycerol (55.0 g initial + 157.0 g fed via 0.200 L of the 785.0 g/L clarified CBG stock, minus 0.8 g residual), achieving a cumulative yield of 0.463 ± 0.017 g/g and a volumetric productivity of 0.905 g/L/h. Relative to the redox-neutral theoretical maximum for glycerol + $CO_2$ → succinic acid (1.0 mol/mol = 1.282 g/g), the 42 °C runs achieved 37.9 % (pure glycerol) and 36.1 % (CBG) of the stoichiometric ceiling, with the remaining substrate carbon partitioned into biomass (27.5 % and 26.8 %) and respiratory $CO_2$ closure (22.0 % and 24.3 %; Table S4).

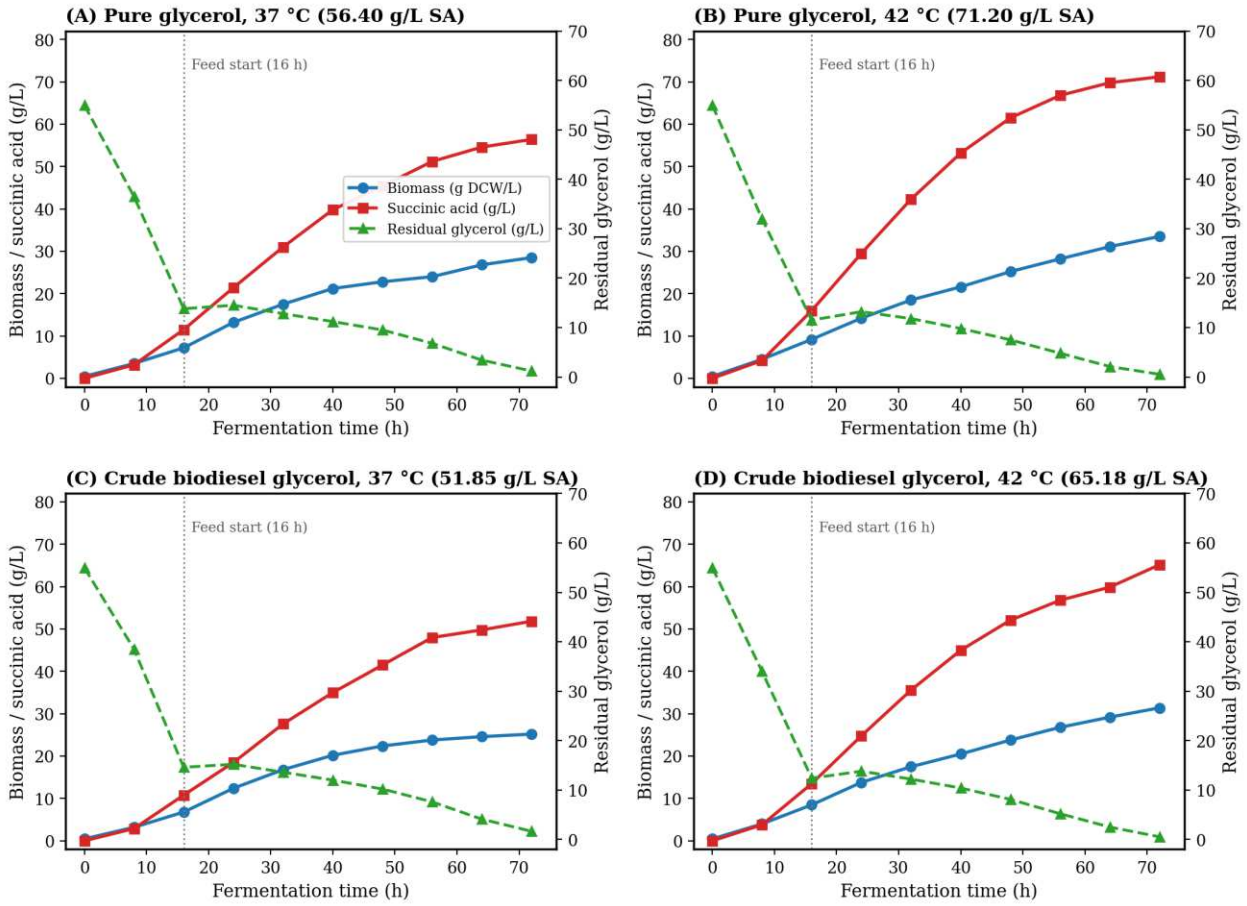



**Fig. 7** Fed-batch fermentation of KM-G08 in a 2.5 L stirred-tank bioreactor at pH 3.65 (titrated with 3.0 M KOH). Pure glycerol at 37 °C (A, 56.40 g/L) and 42 °C (B, 71.20 g/L); pretreated crude biodiesel glycerol (CBG, fed as 785.0 g/L clarified stock) at 37 °C (C, 51.85 g/L) and 42 °C (D, 65.18 g/L). Concentrated glycerol feeding began at 16 h (vertical dotted line) when initial glycerol (55.0 g/L) declined below 15 g/L. Profiles show biomass (blue circles, g DCW/L), succinic acid (red squares, g/L) and residual glycerol (green triangles, dashed line, g/L). Values are mean ± SD (n = 3)

## 4. Discussion

Transitioning succinic acid biomanufacturing from refined sugars to agro-industrial residues requires microbial hosts that combine pathway selectivity with thermotolerance, low-pH tolerance and inhibitor resilience (Nielsen and Keasling 2016; Straathof 2014). Table S2 benchmarks KM-SA06 and KM-G08 against established bacterial and yeast platforms. Metabolically engineered *E. coli* has achieved high molar yields (1.5 mol/mol glucose, 0.98 g/g) under anaerobic neutral-pH conditions by coupling the pentose phosphate pathway with a soluble transhydrogenase (Zhu et al. 2014), while natural and engineered rumen bacteria reach high titres and productivities 90.68 g/L at 0.75 g/g (3.49 g/L/h) in M. succiniciproducens titrated with $Mg(OH)_2/NH_4OH$ at pH 6.5 (Choi et al. 2016) and 98.6 g/L at 0.87 g/g (4.29 g/L/h) in *C. glutamicum* at pH 7.0 on corn stalk hydrolysate (Mao et al. 2018). However, bacterial platforms require neutral pH (6.5-7.0), rich nutrient supplementation and strict mesophilic temperature control, generating stoichiometric salt streams during downstream free-acid recovery (Beauprez et al. 2010; López-Garzón and Straathof 2014). Among yeasts, *S. cerevisiae* remains restricted to 3.6-13 g/L (Ito et al. 2014; Raab et al. 2010), whereas engineered *Yarrowia lipolytica* has reached 160.0 g/L on crude glycerol at pH 6.0 (Gao et al. 2016) and 110.7 g/L at 0.53 g/g without pH control (Cui et al. 2017); nevertheless, *Y. lipolytica* is strictly mesophilic (28–30 °C) and incurs the full mechanical chilling penalty at commercial scale. Low-pH organic acid production at elevated temperature has previously been explored in *Pichia kudriavzevii* for itaconic and D-xylonic acids (Sun et al. 2020; Toivari et al. 2013), whereas high-titer succinic acid production at 42 °C and pH 3.65 had not previously been demonstrated in *K. marxianus*.

The present study does not claim a higher absolute titre than *Y. lipolytica* or rumen bacteria; rather, it establishes a distinct operating window simultaneous 42 °C and pH 3.65 fermentation on detoxified bagasse hemicellulose hydrolysate (58.42 g/L) and crude biodiesel glycerol (65.18 g/L) and quantifies its trade-offs transparently. On carbohydrates, the fed-batch yield of 0.379 g/g represents 33.7 % of the 1.124 g/g redox-balanced sugar ceiling (29.0 % of the 1.311 g/g carbon-only ceiling). Two biological factors account for this yield gap. First, no exogenous $CO_2$ or carbonate salt was sparged into the reactor (air was used as the sole sweep gas), and at pH 3.65 and 42 °C the equilibrium dissolved $CO_2/HCO_3^-$ concentration in air-sparged broth is low (<15 µM bulk, supplemented locally by intracellular respiratory $CO_2$ evolution), whereas A. succinogenes PEPCK exhibits a millimolar Km for $HCO_3^-$; enriching the inlet gas with 5-10 %

$CO_2$ or co-expressing a high-affinity carbonic anhydrase represents a direct route to pull more PEP into OAA. Second, because *K. marxianus* is a respiratory Crabtree-negative yeast, deleting KmADH1, KmGPD1, KmSDH1 and KmACH1 diverted ~39-42 % of sugar carbon into mitochondrial respiration (Table 2 and Table S4), which supplies the ATP required for plasma-membrane proton extrusion against the pH 3.65 gradient (where 78.2 % of extracellular succinic acid is undissociated and permeable to passive back-diffusion).

On the process side, two utility and waste advantages offset the moderate yield. First, operating at 42 °C against a 33 °C cooling-tower supply eliminates the mechanical vapour-compression chiller required at 30 °C (saving 113.7 $kWh_e$/t broth, or 3.41 GWh/year and 1,982 t $CO_2$-eq/year for a 1,000 $m^3$ fermenter) and reduces cooling-tower water circulation by 20.9 % (74.3 vs 93.9 $m^3$/t; Table S5). Second, maintaining the broth at pH 3.65 (where 78.23 % of succinic acid is already protonated as $H_2Suc$) with KOH titration reduces base consumption and subsequent $H_2SO_4$ acidification demand by 78.0 % (0.220 vs 1.958 eq/mol at pH 7.0) and eliminates solid calcium sulfate (gypsum) precipitation completely (0 vs 1,458 kg $CaSO_4 \cdot 2H_2O$/t succinic acid). Unlike insoluble gypsum sludge, the small soluble potassium sulfate fraction generated upon acidifying the 21.8 % dissociated potassium succinate fraction (162–224 kg $K_2SO_4$/t succinic acid) remains in the aqueous mother liquor, avoiding solid-liquid gypsum filtration and offering recovery as a high-value chloride-free potassium fertiliser or closed-loop KOH regeneration via bipolar membrane electrodialysis (Datta and Henry 2006; López-Garzón and Straathof 2014).

## 5. Conclusions

*Kluyveromyces marxianus* was metabolically engineered to produce succinic acid at 42 °C and pH 3.65 from sugarcane bagasse hemicellulose hydrolysate and crude biodiesel glycerol. Combining the cytosolic rTCA pathway (AsPCK, CgMDH, KmFUM1, TbFRD and SpMAE1) with sequential CRISPR/Cas9 deletion of KmADH1, KmGPD1, KmSDH1 and KmACH1 raised product-carbon selectivity from 7.0 to 64.3 % C-mol, converted net acetate excretion into net uptake of 2.06 g/L feedstock acetate, and nearly doubled the shake-flask titre on hydrolysate (2.51 to 4.96 g/L). Pairing an AcXI-based pentose module with non-calcium Amberlite XAD-16N resin detoxification enabled 2.5 L fed-batch bioreactors at 42 °C and pH 3.65 to reach 58.42 g/L succinic acid on bagasse hydrolysate at a yield of 0.379 g/g and a productivity of 0.811 g/L/h. Reconstructing glycerol assimilation through KpGDH and KmDAK1 expanded the whole-cell

NADH pool by 145.2 % and delivered 71.20 g/L succinic acid on pure glycerol (0.486 g/g) and 65.18 g/L on clarified crude biodiesel glycerol (0.463 g/g). Titration with KOH at pH 3.65 eliminates solid gypsum waste (0 vs 1,458 kg/t) and cuts base/acid stoichiometry by 78.0 %, while 42 °C fermentation removes mechanical chilling (113.7 $kWh_e$/t broth) and lowers cooling-water demand by 20.9 %. Future work should address $CO_2$ gas enrichment, adaptive laboratory evolution for pH < 3.0 tolerance, and closed-loop electrodialysis recovery (Cheng et al. 2012; Choi et al. 2015).

## Statements and Declarations


### Funding

This research did not receive any specific grant from funding agencies in the public, commercial, or non-profit sectors.


### Competing Interests

The authors declare no competing interests.

### Data Availability

All data generated or analysed during this study are included in this published article and its supplementary information files (Tables S1–S5).

### Author Contributions

Ashokkumar Kumaravel - Conceptualization, Methodology, Investigation, Data curation, Formal analysis, Visualization, Writing – original draft, Writing – review & editing. Likha Chandran - Writing – review & editing. Prasad Shanmughan - Writing – review & editing.

## References


Abdel-Banat BMA, Hoshida H, Ano A, Nonklang S, Akada R (2010) High-temperature fermentation: how can processes for ethanol production at high temperatures become superior to the traditional process using mesophilic yeast? Appl Microbiol Biotechnol 85:861–867. https://doi.org/10.1007/s00253-009-2248-5

Baptista M, Domingues L (2022) *Kluyveromyces marxianus* as a microbial cell factory for lignocellulosic biomass valorisation. Biotechnol Adv 60:108027. https://doi.org/10.1016/j.biotechadv.2022.108027

Beauprez JJ, De Mey M, Soetaert WK (2010) Microbial succinic acid production: natural versus metabolic engineered producers. Process Biochem 45:1103–1114. https://doi.org/10.1016/j.procbio.2010.03.035

Borges ER, Pereira N (2011) Succinic acid production from sugarcane bagasse hemicellulose hydrolysate by *Actinobacillus succinogenes*. J Ind Microbiol Biotechnol 38:1001–1011. https://doi.org/10.1007/s10295-010-0874-7

Bozell JJ, Petersen GR (2010) Technology development for the production of biobased products from biorefinery carbohydrates: the US Department of Energy's 'Top 10' revisited. Green Chem 12:539–554. https://doi.org/10.1039/b922014c

Cheng KK, Zhao XB, Zeng J, Zhang JA (2012) Biotechnological production of succinic acid: current state and perspectives. Biofuels Bioprod Biorefin 6:302–318. https://doi.org/10.1002/bbb.1327

Choi S, Song CW, Shin JH, Lee SY (2015) Biorefineries for the production of top building block chemicals and their derivatives. Metab Eng 28:223–239. https://doi.org/10.1016/j.ymben.2014.12.007

Choi S, Song H, Lim SW, Kim TY, Ahn JH, Lee JW, Lee MH, Lee SY (2016) Highly selective production of succinic acid by metabolically engineered *Mannheimia succiniciproducens* and its efficient purification. Biotechnol Bioeng 113:2168–2177. https://doi.org/10.1002/bit.25988

Cui Z, Gao C, Li J, Hou J, Lin CSK, Qi Q (2017) Engineering of unconventional yeast *Yarrowia lipolytica* for efficient succinic acid production from glycerol at low pH. Metab Eng 42:126–133. https://doi.org/10.1016/j.ymben.2017.06.007

Datta R, Henry M (2006) Lactic acid: recent advances in products, processes and technologies — a review. J Chem Technol Biotechnol 81:1119–1129. https://doi.org/10.1002/jctb.1486

Gao C, Yang X, Wang H, Rivero CP, Li C, Cui Z, Qi Q, Lin CSK (2016) Robust succinic acid production from crude glycerol using engineered *Yarrowia lipolytica*. Biotechnol Biofuels 9:179. https://doi.org/10.1186/s13068-016-0597-8

Haeussler M, Schönig K, Eckert H, Eschstruth A, Mianné J, Renaud JB, Schneider-Maunoury S, Shkumatava A, Teboul L, Kent J, Joly JS, Concordet JP (2016) Evaluation of off-target and on-target scoring algorithms and integration into the guide RNA selection tool CRISPOR. Genome Biol 17:148. https://doi.org/10.1186/s13059-016-1012-2

Hsu PD, Scott DA, Weinstein JA, Ran FA, Konermann S, Agarwala V, Li Y, Fine EJ, Wu X, Shalem O, Cradick TJ, Marraffini LA, Bao G, Zhang F (2013) DNA targeting specificity of RNA-guided Cas9 nucleases. Nat Biotechnol 31:827–832. https://doi.org/10.1038/nbt.2647

Ito Y, Hirasawa T, Shimizu H (2014) Metabolic engineering of *Saccharomyces cerevisiae* to improve succinic acid production based on metabolic profiling. Biosci Biotechnol Biochem 78:151–159. https://doi.org/10.1080/09168451.2014.877816

Jönsson LJ, Martín C (2016) Pretreatment of lignocellulose: formation of inhibitory by-products and strategies for minimizing their effects. Bioresour Technol 199:103–112. https://doi.org/10.1016/j.biortech.2015.10.009

Lane MM, Morrissey JP (2010) *Kluyveromyces marxianus*: a yeast emerging from its sister's shadow. Fungal Biol Rev 24:17–26. https://doi.org/10.1016/j.fbr.2010.01.001

Ledesma-Amaro R, Lazar Z, Rakicka M, Guo Z, Fouchard F, Crutz-Le Coq AM, Nicaud JM (2016) Metabolic engineering of *Yarrowia lipolytica* to produce chemicals and fuels from xylose. Metab Eng 38:115–124. https://doi.org/10.1016/j.ymben.2016.07.001

Li Q, Wang D, Wu Y, Li W, Zhang Y, Xing J, Su Z (2010) One step recovery of succinic acid from fermentation broths by crystallization. Sep Purif Technol 72:294–300. https://doi.org/10.1016/j.seppur.2010.02.021

López-Garzón CS, Straathof AJJ (2014) Recovery of carboxylic acids produced by fermentation. Biotechnol Adv 32:873–904. https://doi.org/10.1016/j.biotechadv.2014.04.002

Mao Y, Li G, Chang Z, Tao R, Cui Z, Wang Z, Tang YJ, Chen T, Zhao X (2018) Metabolic engineering of *Corynebacterium glutamicum* for efficient production of succinate from

lignocellulosic hydrolysate. Biotechnol Biofuels 11:95. https://doi.org/10.1186/s13068-018-1094-z

Nielsen J, Keasling JD (2016) Engineering cellular metabolism. Cell 164:1185–1197. https://doi.org/10.1016/j.cell.2016.02.004

Nonklang S, Abdel-Banat BMA, Cha-aim K, Moonjai N, Hoshida H, Limtong S, Yamada M, Akada R (2008) High-temperature ethanol fermentation and transformation with linear DNA in the thermotolerant yeast *Kluyveromyces marxianus* DMKU3-1042. Appl Environ Microbiol 74:7514–7521. https://doi.org/10.1128/aem.01854-08

Raab AM, Gebhardt G, Bolotina N, Weuster-Botz D, Lang C (2010) Metabolic engineering of *Saccharomyces cerevisiae* for the biotechnological production of succinic acid. Metab Eng 12:518–525. https://doi.org/10.1016/j.ymben.2010.08.005

Straathof AJJ (2014) Transformation of biomass into commodity chemicals using enzymes or cells. Chem Rev 114:1871–1908. https://doi.org/10.1021/cr400309c

Sun W, Vila-Santa A, Liu N, Prozorov T, Xie D, Faria NT, Ferreira FC, Mira NP, Shao Z (2020) Metabolic engineering of an acid-tolerant yeast strain *Pichia kudriavzevii* for itaconic acid production. Metab Eng Commun 10:e00124. https://doi.org/10.1016/j.mec.2020.e00124

Toivari M, Vehkomäki ML, Nygård Y, Penttilä M, Ruohonen L, Wiebe MG (2013) Low pH D-xylonate production with *Pichia kudriavzevii*. Bioresour Technol 133:555–562. https://doi.org/10.1016/j.biortech.2013.01.157

Wang R, Li L, Zhang B, Gao X, Wang D, Hong J (2013) Improved xylose fermentation of *Kluyveromyces marxianus* at elevated temperature through construction of a xylose isomerase pathway. J Ind Microbiol Biotechnol 40:841–854. https://doi.org/10.1007/s10295-013-1282-6

Yuzbashev TV, Yuzbasheva EY, Sobolevskaya TI, Laptev IA, Vybornaya TV, Larina AS, Matsui K, Fukui K, Sineoky SP (2010) Production of succinic acid at low pH by a recombinant strain of the aerobic yeast *Yarrowia lipolytica*. Biotechnol Bioeng 107:673–682. https://doi.org/10.1002/bit.22859

Zhu X, Tan Z, Xu H, Chen J, Tang J, Zhang X (2014) Metabolic evolution of two reducing equivalent-conserving pathways for high-yield succinate production in *Escherichia coli*. Metab Eng 24:87–96. https://doi.org/10.1016/j.ymben.2014.05.003

## Supplementary Files

This is a list of supplementary files associated with this preprint. Click to download.

- V3SupplementaryWJMB.docx